SAPIENZA
UNIVERSITÀ DI ROMA

Sarah Modesti

PhD Thesis in Biophysics
XXIV Cycle (2008-2010)

CHARACTERIZATION OF BIOLOGICALLY EFFECTIVE UV RADIATION AT MID-LATITUDES SITES: INNOVATIVE METHOD FOR THE CALCULATION OF THE HUMAN VITAMIN D EXPOSURE

PHD COORDINATOR:

PROF. ALFREDO COLOSIMO

PHD SUPERVISOR:

DR. ANNA MARIA SIANI

PROF. ALFREDO COLOSIMO

to Fabrizio

to my Parents

Acknowledgments

This work has been carried out at the G-Met, Dept. of Physics, Sapienza University of Rome.

I wish to express my sincere gratitude to:

My supervisor, **Dr. Anna Maria Siani** (Dept. of Physics, Sapienza Univ. of Rome) her teaching and dedication to Science. This study would not have been possible without the precious experience and knowledge of Anna Maria on this topic.

My Phd Coordinator and Supervisor, **Prof. Alfredo Colosimo** (SAIMLAL Dept., Sapienza Univ. of Rome) for his teaching and guidance.

I am particularly grateful to **Anna Maria** and to **Prof. Colosimo** for the long hours they spent to guide me and check my work.

Dr. Giuseppe Rocco Casale (Dept. of Physics, Sapienza Univ. of Rome), who shared with me his deep knowledge in

the “art of polysulphone”. His support has been determinant for many aspects of my work.

Dr. Henri Dièmoz (ARPA VDA), who shared with me the Aosta data and has always been available to discuss with me their relevance with respect to my work.

Dr. Iolanda Ialongo (Finnish Meteorological Institute), whose PhD thesis has represented a basis for my work.

Virginia, my Senior PhD collegue and dear friend, who initiated me to the “art of programming” using IDL.

Valerio, Cecilia, Giampietro, Annamaria, PhD collegues and friends, with whom I shared problems, hopes and amiable hours in the Department

Foreword

Although the Italian territory has the potential for receiving high UV doses most of the year, and Italy immediately follows Australia and USA for melanoma skin cancer incidence, a climatological characterization of biologically effective UV radiation in our Country is missing as well as any appropriate legislation or governmental program regarding UV exposure of the population with outdoor lifestyle (leisure /working activity). Moreover, little knowledge and/or indifference about an appropriate 'sun-behaviour' has been verified by a recent large scale survey on the web (1).

In such a context, an additional point worth of consideration is the well-established beneficial effect of solar ultraviolet radiation on the skin due to the enhanced synthesis of pre-vitamin D_3. Solar radiation in the UVB waveband photo-chemically converts 7-dehydrocholesterol in the epidermis to pre-vitaminD_3, which is then converted to vitaminD_3 (see Figure1).

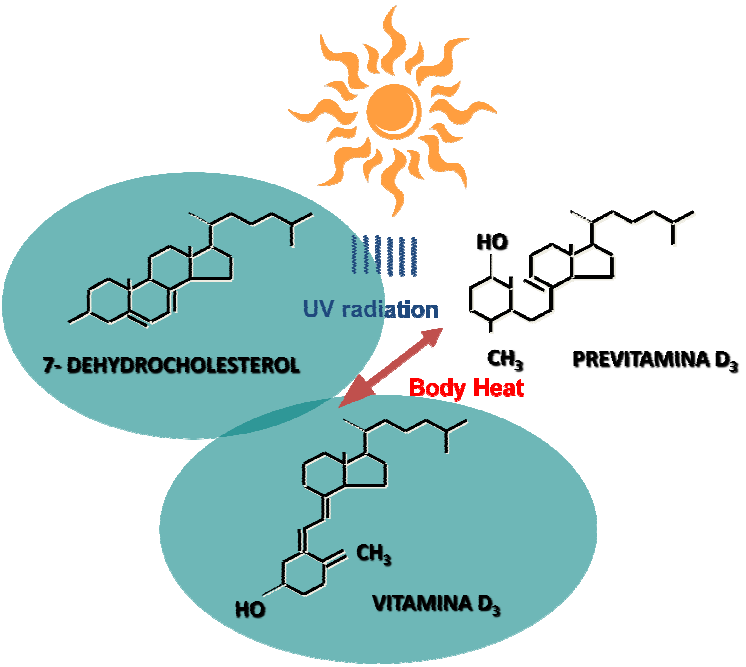

Figure 1 Photoproduction of Vitamin D by UV Radiation (by courtesy of (2)).

Sunlight also regulates and limits further production of vitaminD_3 in the skin to preclude a toxic level (3) (4). Vitamin D plays an essential role in the body's proper uptake of calcium, which is important for bone and musculoskeletal health. In addition, there is evidence of an increased risk of autoimmune diseases, including multiple sclerosis, type-1 diabetes and rheumatoid arthritis with low vitamin D intake or low UV exposure. Some recent epidemiological studies suggest a link between abnormal cell proliferation and low

vitamin D levels and several recent studies suggested the possible protective role of vitamin D in other diseases and even in some neoplasias of internal organs (5) (6) (7).

Around midday in the tropics, and in Spring and Summer in more temperate climates, only brief sub-erythemal exposures to sunlight are required to synthesize vitamin D_3. In this case, less than 15 minutes of solar UVR exposure on the hands, arms and face fulfils this requirement. However, at high latitudes outside the tropics, there may be insufficient ambient UVB in the winter for this process, with a greater negative impact for elderly people or persons having highly pigmented skin (3).

All in all, the duality of UV radiation on human health calls for a better knowledge of the many facets of a such relevant issue in order to adopt proper sun-behaviour exposure, to maximize vitamin D production, and to reduce harmful effects.

Aims of the study

Given the dual nature of UV radiation, this work is focused on the characterization of erythemal and vitamin D dose rates at two Italian sites with different environmental conditions: Rome (41.9°N,12.5°E, 70 m a.s.l) and Aosta (45.8°N, 7.4°E,

569m a.s.l.). For both sites multi-year series of high quality spectral UV measurements, provided by Brewer spectrophotometers are available, especially at the Rome station which has the longest available spectral measurements of UV irradiances in Italy (more than 15 years). The climatological characterization of erythemal and vitamin D radiation has been carried out in relation to total ozone, solar zenith angles, aerosol optical index and sky conditions. The results of this study can contribute to support the assessment of UV-radiation induced health and environmental risks, and, can be used in the design of prevention strategies and appropriate sun safety protection roles for outdoor activities also ahead of the foreseeable European Union directive in this field.

In addition, the results of the climatological analysis allowed to study the applicability of an innovative method to derive vitamin D doses based on polysulphone dosimetry -- normally used to measure erythemal exposures -- and hence to extend the potential applications of the PS dosimetric technique.

The thesis is structured in 5 chapters.

Chapter 1 gives a comprehensive introductory information on the main factors driving the intensity of UV radiation at the Earth' surface.

Chapter 2 provides a review of UV effect on human health focusing on the erythemal effect and the photoproduction of vitamin D. Particular attention is paid to the parameters affecting personal exposure (skin phototype, age, sunscreen, posture, activities). The photobiological quantities such as dose rates and doses are also described here.

Chapter 3 describes the main techniques to measure ambient UV irradiance and the personal exposure. The data set and the study design are also illustrated .

Chapter 4 reports on the characterization of the biologically effective (erythemal and vitaminD) UV dose rates for the two sites under study: Rome and Aosta. The ratio between the two biologically effective (erythemal and vitaminD_3) UV dose rates are also carefully analyzed in relation to sky conditions (cloudy and cloudless days). To search the ozone-induced variability through the Radiation Amplification Factor the analysis has been restricted to cloud- free atmosphere. Further analysis is performed for three selected hours of the day, for three specific solar zenith angles (SZA), for fixed range of total ozone values, and finally for fixed aerosol index (AI) values. Following the results of the ratios in both sites, the calculation of exposure time to induce erythema and for the

photoproduction of vitamin D, is provided as a function of the UV index.

New approach for the use of polysulphone (PS) dosimetry to quantify erythemal UV dose as well as to estimate the vitamin D dose is presented. Together with its validation on the basis of data obtained in a number of field campaign.

Chapter 5 This final chapter overviews the findings of the study, discusses the significance of the results and provides useful recommendations for appropriate sun-exposure behaviour.

1 Solar UV Radiation

Introduction

Solar Ultraviolet (UV Radiation) is part of the electromagnetic spectrum with wavelengths shorter than 400nm. The ultraviolet waveband is traditionally included in the non-ionizing radiation although the UV band has enough energy to break the bond of macromolecules (8). It is divided into three bands although the exact wavelength at which the divisions are made differ in accordance with different disciplines (9). The Second International Congress on Light in Copenhagen in 1932 defined three regions: UVA 400-315nm, UVB 315-280nm, UVC 280-100nm. However, in photobiology the boundaries for these regions are slightly different and associated with the biological effects: UVA 400-320nm, UVB 320-290nm, UVC 290-200nm.

1.1 Factors affecting solar UV irradiance at Earth's surface

UV radiation is approximately 9.3% of the total solar radiation at the top of the atmosphere. Of the total amount of UV reaching the Earth's surface approximately 6-7% is in the

UVA region and less than 1% is in the UVB band, while UVC is completely absorbed by ozone and oxygen in the upper atmosphere.

The UV irradiance at surface is usually called global UV and it can be divided into direct and diffuse components. The direct component is the amount of UV radiation that passes through the Earth's atmosphere and it is attenuated by the absorbing gases. Forward and backward scattering (Rayleigh scattering due to gaseous molecules and Mie scattering due to large particles) remove a large amount of UV radiation from the direct beam. Reflection of backward radiation can occur in presence of clouds and can reach the ground by indirect route. Thus, the diffuse component represents radiation incident to the surface from all directions.

The large variability of surface UV radiation is controlled by a combination of several factors that can interact in synergy. They can be divided into: astrophysical (solar irradiance at the top of the atmosphere), astronomical and atmospheric.

The astronomical factors include :

- Earth-sun distance;
- solar zenith angle, which depends on latitude, day of the year and time of the day;

Atmospheric factors are:

- absorption and scattering due to the atmospheric molecules (mainly ozone);
- absorption, scattering and reflection by aerosols;
- clouds.

In addition the characteristics of the site such as altitude above sea level and albedo from the surface and surroundings (reflectivity) are responsible of large geographical surface UV radiation variability.

Although the knowledge of the above factors has been improved in the last decade, there are still large uncertainties on the behaviour of variable atmosphere components (such as clouds and aerosol) and on their influence on the surface UV levels. Even if the predicted gradual stratospheric ozone recovery to the pre-1980 levels occurs in the decades ahead, future UV levels are difficult to assess due to the still limited understanding of the interactions between climate changes and ozone.

1.1.1 Astrophysical and astronomical factors

UV radiation is controlled by the variation in the cyclic Sun emittance. The 27-day cycle leads to variations less than 1%

for λ >250nm, 6-8% in the band 245-250nm. The 11-year sunspot cycle determines small changes in irradiance (less than 0.1%) and influences the shortest extra-terrestrial wavelengths, less than 1% at 300nm. Changes in the UVC band affect the chemical equilibrium of stratospheric ozone and the indirect effect on the transmission of UVB at surface

The most important astronomical factor influencing surface UV radiation is solar elevation (most commonly described by the solar zenith angle (SZA), i.e. the angle between the local zenith and the Sun) (10). The higher the Sun from the horizon (the smaller SZA), the shorter the atmospheric path that radiation crosses, (the lower the attenuation and hence higher UV levels at surface). It should be mentioned that solar UV irradiance on horizontal surface is weighted according to the cosSZA.

Another astronomical factors is the Earth-Sun distance (R_n) which varies about 3.4% from minimum (perihelion, on about Jan 3rd) to maximum (aphelion, on about July 4th). The variation in R_n^2, and therefore in the intensity of extraterrestrial radiation, is about 6.9%, and is significant especially when considering seasonal differences in UV intensities between Southern and Northern Hemispheres.

1.1.2 Atmospheric factors

The main atmospheric absorber of UV radiation is the ozone (O3), which is located predominantly (90%) in the stratosphere. The absorption of solar radiation by ozone is higher at shorter wavelengths, Hartley band (220-310nm), which filters the UVC radiation reaching the surface. Furthermore, most of the solar UVB radiation is absorbed in the Huggins band (310-370nm). Consequently the presence of ozone is crucial for the Earth's biosphere due to the filtering of the biologically hazardous radiations.

Following the discovery of Antarctic ozone hole in 1985 (11), and the significant decrease in total ozone at middle latitudes observed since the 1970s , the ozone has became an important environmental, ecological and atmospheric parameter to be measured and studied. The scientific community has shown a growing concern about the ozone decreases and their effects on human health risks deriving from over-exposure to solar UV radiation.

However ozone is not the only parameter influencing surface UV levels. Cloud transmission can affect largely the UV variability at the surface. Although UV radiation is reduced slightly less than visible radiation by clouds, heavily overcast

conditions can reduce surface UV irradiance by 90%. On average, clouds have an attenuating effect of 15–32% in the UV waveband (12). However in any given situation the cloud effect will depend on the cloud type, depth, and distribution across the sky. Thus, cloud transmission of UV irradiance is difficult to quantify in sufficient detail to provide the determination of its effect at a given time and place (13).

Air pollution, i.e., scattering and absorption by aerosols (black and organic carbon, hydrocarbons, dust, and smoke) as well as absorption by tropospheric O_3, nitrogen dioxide (NO_2), sulfur dioxide (SO_2) and other gases can reduce UV radiation by up to 15% at polluted sites, with reductions greater than 25% in highly polluted cities. The UV response to changes in these gaseous pollutants, may be larger than the UV response to changes in stratospheric ozone. In some locations increased pollution and aerosols may have masked an increase in UV irradiance due to ozone decrease in the 1980s and 1990s, and present cleaner air policies may hide the effect of ozone recovery on UV irradiance.

Black carbon is the main absorbing component present in the lower atmosphere. In addition, soil dust absorbs radiation in the UV and visible wavebands and recently there have been several studies showing enhanced UV absorption due to

organic carbon (14). The sources and formation of these compounds and their temporal variability, however, are currently not well understood (15) (16).

1.1.3 Geographical factors

UV radiation increases with altitude, because of reduction of scattering and absorption by the less-dense overhead atmosphere, and, at higher altitudes, because of additional reflections from the surface and the clouds below. It is assessed that UV radiation levels increase by 6% to 10% every 10^3 m altitude increase. Recent studies have showed that the altitude effect of UV irradiance cannot be described by a single number (i.e not linear) because it depends on a combination of several factors such as reduction of scattering and absorption, clouds effects, tropospheric ozone, albedo (17) (18) and wavelength.

1.1.4 Albedo and Reflectivity

Albedo is defined as the ratio of reflected (upwelling) irradiance to incident (downwelling) irradiance for horizontal surfaces (19). A tilted surface is exposed to downwelling irradiance and can produce reflected irradiance to the nearby environment. The reflectivity cannot be assumed equivalent to

albedo as it is dependent on the reflecting surface orientation and direction as well as on solar zenith angle and type of surface.

The UV irradiance over a high-albedo surface is greater than that above a snow-free surface, and this effect can be further enhanced by cloudiness and by the multiple reflections between snow and cloud surfaces (20). The albedo for snow-covered surfaces varies with snow type and age, and can approach unity for fresh, pure snow (20) (21). Changes in the extent and seasonality of snow cover due to climate change could thus lead to large surface UV variations.

1.2 Measurements of ambient UV radiation

The variability of surface UV irradiance in time and space can either be inferred from direct measurements (from ground or space) or reconstructed by mean of radiative transfer models using as proxy data total ozone and sun shine duration.

There are three types of ground-based systems employed in the measurements of UV: broad-band and narrow –band radiometers and spectroradiometers. These instruments usually measure the radiation incident on an horizontal surface with a hemispheric field of view. Radiometers and

spectroradiometers are both direct-reading instruments that use electro-optical detectors to convert the incident radiation into an electrical signal. Radiometers measure all incident radiant power over a selected spectral band; spectroradiometers provide spectral radiometric quantities directly, such as spectral irradiance or spectral radiance.

The satellite techniques have been developed to measure ozone and UV in the atmosphere, and are essential in order to obtain data with a large geographical coverage.

Significant advancements have been reported in the last few years in measurements and calibration procedures of instruments and in algorithms used by both ground-based and satellite-borne platforms (22).

2 Biological Effects of UV Radiation

Introduction

In photobiology, the concept of a biologically effective dose is of critical importance. Solar UV radiation reaching the Earth surface is responsible of a variety of different effects on biological systems. The effectiveness of UV radiation in causing a specific reaction within a biological system usually is described by weighting functions (or action spectrum) in order to define the relative effectiveness of different wavelengths. A number of “main” action spectra which have been used in a wide range of studies concerning DNA damage (23) (24), erythema (25) (26), squamous cell carcinoma in mice, malignant melanoma in fish and plant damage (27) (28), and the associated response curve is generally normalized to unity at the wavelength of maximal sensitivity. The "biologically effective solar exposure", or "biologically effective dose” is the incident weighted irradiance on a given surface (dose rate in W per square meters) over a specified period of time, expressed in Joules per square meters.

Prolonged human exposure to solar UV radiation may result in acute and chronic health effects on skin, eyes and immune system. Sunburn and tanning are the best known acute response to excessive UV radiation exposure; chronic and lifetime sun exposure induce

degenerative changes in cells, fibrous tissue and blood vessels and lead to premature skin ageing. UV radiation can also cause inflammatory reactions of the eye, such as photokeratitis. Chronic effects include cutaneous malignant melanoma (CMM) and non melanoma (NMSC) skin cancers (20% are squamous cell carcinomas and 80% are basal cell carcinomas in fair-skinned populations), the most common cancer type worldwide.

However, small amounts of UV radiation are beneficial for people and essential in the production of vitamin D. UV radiation is also used to treat several diseases, including rickets, psoriasis and eczema (29).

2.1 Skin sunburn

The best known acute effect of excessive UV radiation exposure is erythema, the familiar skin reddening termed sunburn, usually assessed at 24 h after exposure, which is highly dose and wavelength dependent. The erythema results from an increased blood content near the skin's surface. Higher doses may result in pain and skin swelling (edema) with blistering, and after a few days, peeling. The erythemal response depends not only on the UV dose but also on skin type. Individual sensitivity to sunburn is usually defined by the minimal erythema dose (MED) being the minimum dose that will produce a just perceptible erythema 8-24 hours after irradiation of

the skin. It is worth reminding that MED is not a standardized quantity but an individual measure of susceptibility to sunburn that accounts for skin type differences. The Fitzpatrick skin classification (30) is reported in Table 1. Thus the CIE Standard Erythemal Dose (SED) was introduced, defined as an erythemal effective exposure equivalent to 100 J/m^2 (25).

In the last decades a dimensionless UV index, between 1 and 12 (or more in specific cases) was introduced, (26) used for public health information about the potential detrimental effects on health from overexposure to UV radiation. A UVI of 1.0 is slightly less than one SED per hour. However, the UV index is of limited value because specific anatomical sites can be overexposed receiving much higher UV doses than those provided by UV index (31) (32).

Skin type	Description	SED
I	Celtic (always burn)	2 - 3
II	Pale (burns easily)	2.5 - 3
III	Caucasian (may burn)	3 – 5
IV	Mediterranean (burns rarely)	4.5 – 6
V	S. American (rarely burns)	6 – 20
VI	Negroid (rarely burns)	6 - 20

Table 2.1 Skin type classifications according to the Fitzpatrick scale (30).

2.2 Suntanning and skin ageing

Delayed tanning (melanogenesis) and immediate pigment darkening are the skin response to UV radiation.

Skin adaptation from frequent UV exposure is also characterized by skin thickening of the outermost layers of the skin (epidermis and stratum corneum). This can be a 3 to 5-fold thickening of the stratum corneum within one to seven weeks after several UV exposures and returns to normal about one to two months after ceasing exposure. This thickening leads to a significant increase in UV protection by a factor of five or greater, and in lightly pigmented skin types, thickening is probably more important than tanning in providing protection. The wavelengths of the radiation that induce tanning are very similar to those of radiation producing erythema.

Chronic UV exposure leads to photoaging which has traditionally been particularly observed in outdoor workers who receive regularly substantial solar UV exposure such as agricultural workers, ski resort guides, lifeguards and fishermen mainly on the face and the back of the neck and hands. The clinical signs of a photo-aged skin are dryness, deep wrinkles, accentuated skin furrows, sagging, loss of elasticity, mottled pigmentation and the development of tiny but highly visible, superficial blood vessels. It is not yet clear which wavelengths are the most responsible for photoaging, but some

research studies (33) (34) (35) indicate solar UVA and even infrared radiation exposures as contributing factors.

2.3 Skin cancers

Evidence indicates that chronic and cumulative lifetime sun exposure is the strongest environmental risk factor associated to skin cancers. According to the World Health Organization (36) excessive solar UVR exposure caused 60,000 premature deaths per year worldwide, 48,000 were caused by cutaneous malignant melanoma (CMM) and 12,000 were related to non melanoma skin cancers (NMSC). The latter group comprises basal cell carcinoma (BCC) and squamous cell carcinoma (SCC). BCC is the most common type in the fair population. Incident rates increases with age, however BCC can occur in people as young as their 20s. SCC account for about one-third of skin cancers. It can develop quickly over a period of weeks to months It appears on skin most often exposed to the sun. As BCC incident rates increase with age, thus it tends to occur from the age of 40 onwards. It is not as dangerous as melanoma, but it can spread to other parts of the body if left untreated.

Malignant melanoma is most aggressive form of skin cancer and grow and spread rapidly. It can start in normal looking skin, or in a freckle or mole and can develop anywhere in the body - not just areas exposed to the sun.

2.4 Eye damage

The eye is recessed within its orbit and shielded by the brow ridge, eyebrows and eyelashes. Bright light activates the constriction of the pupil and the squinting reflex to minimize the penetration of the sun's rays into the eye. However, the effectiveness of these natural defenses in protecting against the dangers of UV radiation is limited under extreme conditions such as sunbed use or strong ground reflection from sand, water and snow. Acute effects of UV radiation exposure include photokeratitis and photoconjunctivitis (37). These inflammatory reactions are comparable to a sunburn of the very sensitive skin-like tissues of the eyeball and eyelids, and usually appear within a few hours of exposure (38). High intensity exposure lead "arc-eye" and "snow blindness". Cataracts are the leading cause of blindness in the world. Proteins in the eye's lens unravel, tangle and accumulate pigments that cloud the lens and eventually lead to blindness. Even though cataracts appear to different degrees in most individuals as they age, sun exposure, in particular exposure to UVB, appears to be a major risk factor for cataract development (39).

2.5 Immunodepression

Through photochemical reactions, UV radiation can alter various organic molecules in the skin and these molecules may become dysfunctional and 'foreign' to the skin (40). An important task of the

body's immune system is to seek out and destroy any "foreign intruders," and it is therefore conceivable that UV radiation could trigger unwanted immune reactions against the skin (this might actually cause 'sun allergy') (41). It has, however, been established that UVB exposure reduces specific immune reactions in the skin of healthy people and this is likely to constitute a healthy response to avoid any undesired immune reaction against the UV exposed skin (37). This effect is usually only temporary, but it can have clear drawbacks when it coincides with an infection or with abnormal cell growth. For these conditions, UV exposure of the affected area should be minimized. Not only infections in the skin can be aggravated, but also internal infections. The common 'cold sore' that is evoked by sun exposure appears to be a good example of an infection (by stimulating the Herpes simplex virus) in humans brought forth by UVB exposure. In all, there is much evidence that UV radiation affects immunity and, because of that, can aggravate infections and allow the development of (skin) cancers (42).

2.6 Beneficial Effects

The best-established beneficial effect of solar ultraviolet radiation on the skin is the synthesis of vitamin D_3 (43). Vitamin D is known to be essential for the body's proper uptake of calcium, which is important for bone and musculoskeletal health. Recent studies indicate that it may have also several other health benefits such as

prevention or mitigation of cancer (44) and autoimmune diseases (45), reduction in hypertension (46), a positive regulatory effect on the immune system and prevention of influenza (47). On the contrary a long-term vitamin D deficiency may induce a wide range of harmful biological effects.

The usual measure of vitamin D status is the circulating concentration of 25-hydroxyvitamin D (25(OH)D), which incorporates both vitamins D_2 and D_3 from the diet and vitamin D_3 from sun exposure. The formation, intake and circulation of vitamin D are outlined in Figure 1. provitamin D (7-dehydrocholesterol, 7-DHC) is converted to previtamin D in the skin by exposure to UVB radiation. The previtamin D is then isomerized by body heat to form vitamin D_3. Vitamin D_3 is then transported by the blood to the liver, where it is converted to 25-hydroxyvitamin D (25(OH)D). In the kidneys, the formation of the active form of vitamin D, 1,25-dihydroxyvitamin D (1,25(OH)2D), tightly regulated by the parathyroid hormone (PTH), is important for the uptake of calcium and mobilization of calcium stores. Many organs have receptors for vitamin D, and consequently vitamin D is important for many bodily functions. Although the underlying processes of vitamin D synthesis and circulation is known, the quantitative relationship of UV exposure to humans and the resulting vitamin D production is inadequately explained. The search for an optimal UV exposure is a subject of ongoing debate (44) (48) (49).

As for erythemal effect also for pre-vitaminD_3 a standard vitamin D dose (1 SDD) for each skin types can be defined based on exposure of 1/4 body surface area and it corresponds to the UV equivalent of an oral dose of about 1000 IU vitamin D (50).

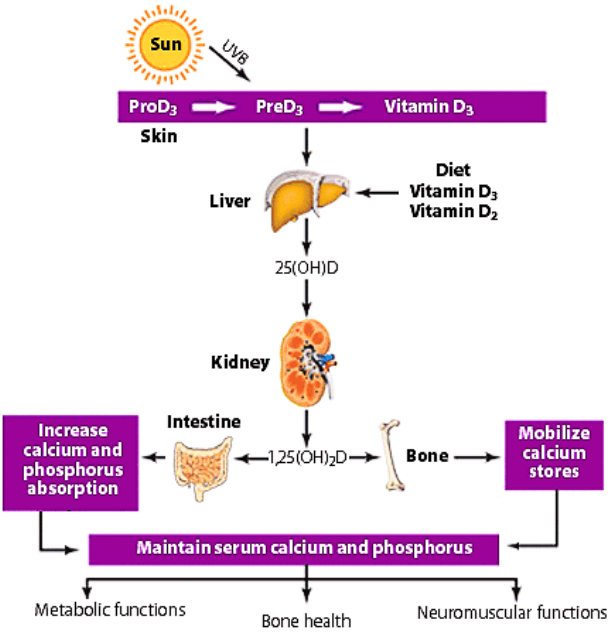

Figure 2.1 Outline of vitamin D synthesis and metabolism. By courtesy of (51).

2.7 Factors that Influence Human Exposure to Solar UVR

Humans have evolved in sunlight environment , leading to different skin pigmentation: darker skin pigmentation for people at low latitudes to offer protection from deleterious effects; fair skin for those at higher latitudes to maximize positive effects.

Anatomical sites are differently exposed and receive levels of UV radiation which can be higher than levels received from horizontal surfaces. The individual UV exposure (personal exposure) depends on ambient UV radiation which in turn depends on environmental characteristics (urban areas, mountains, marine sites) as well as to a variety of factors like:

- skin type (see Table 1);
- the orientation of the exposed anatomical site during the outdoor activity;
- time of exposure;
- the architectural and natural environment that cause shadow;
- use of sun protection (sunglasses, goggles, hats, clothing and sunscreens).

Regarding the latter issue it is to bear in mind that total sunscreen can block UVB radiation and then could affect the vitamin D

production (37). In addition at cold temperatures the population wears more clothes for comfort, reducing the skin area to UVB radiation, and thereby inhibiting vitamin D synthesis (52) (53). Furthermore it was observed that overweight individuals have reduced capacity of vitamin D synthesis (54) and elderly people have thinner skin, and consequently are less capable of synthesizing vitamin D in their skin (55).

Figure 2.2 shows the main factors which affect ambient UVR at Earth surface and the individual factors which affect personal exposure and the associated diseases (36).

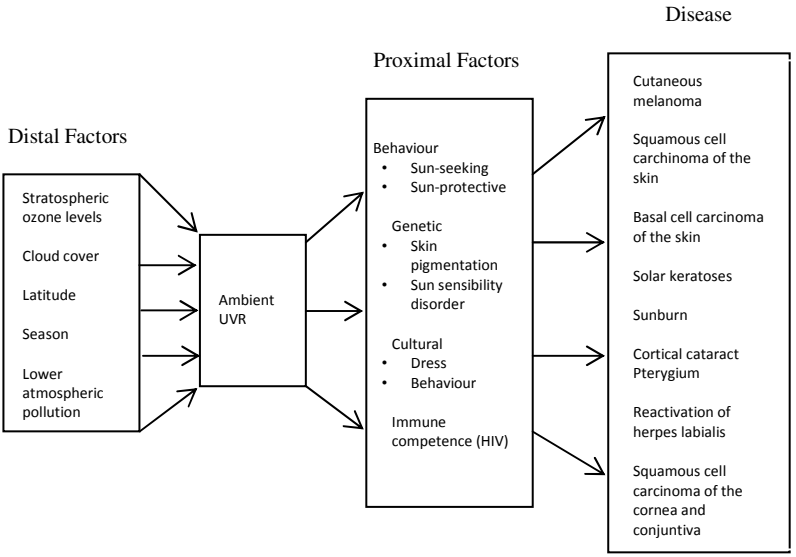

Figure 2.2 Causal Web for Health Impacts due to Ultraviolet Radiation (by courtesy of (36)).

2.8 Main techniques to measure personal exposure

Dosimetry (chemical, biological and electronic) is employed to assess the personal doses received by selected anatomical sites during different postures under several environmental conditions. The most widely used UV dosimeters are polysulphone (PS) films which have a response to UV radiation similar to human skin (56) (57) (58) (59). The PS method is based on the measurements of optical absorbance changes which increases as result of the UV absorbed dose (mainly in the UVB portion of the spectrum). However such technique does not allow recording of cumulative long time doses. More details on PS dosimetry are given in chapter 3.

3 Materials and Methods

3.1 Ground based UV and ozone measurements

3.1.1 Ambient UV irradiance

There is a scarce availability of UV datasets longer than 15 year worldwide (60). The coverage of UV monitoring stations is sparse with large areas of land surface with no UV instrumentation and no UV measurements refer to oceanic regions are available. Direct measurements of UV radiation started in the 1990s while satellite UV products have been available since 1979 (61). Recently reconstructed ambient erythemal dose in the past (1958-2001) over Europe were carried out within the COST ACTION 726 (Long Term Changes and the Climatology of UV radiation over Europe) (62). To reconstruct the UV irradiance reaching the Earth's surface radiative transfer calculations and statistical models are used. However, uncertainties in the model input parameters yield uncertainties in the model outputs of about 6% for clean sites, and up to 20% for sites with very large aerosol load (63) (64). Hence the need of ambient solar UV radiation measurements in order to evaluate the influence of atmospheric composition changes on solar UV irradiance at the ground is increased (61). It is also important to achieve a more reliable assessment of people UV exposures considering that the

IARC (International Agency for Research on Cancer) has recently confirmed solar UV as carcinogenic to humans (65). Consequently the accuracy, both in developing and maintaining the instruments, in data processing and calibration procedures, and in quality assurance and quality control (QA/QC) methods are mandatory for a reliable ozone and UV trend detection, mainly in urban sites and for the validation of satellite measurements (66) (67) (61). The latitude extension and the variety of environmental conditions representative of the Mediterranean as well as of the Alpine regions (68), make solar UV measurements in Italy an important issue (22).

In the present study high-quality UV irradiance measurements at two Italian sites have been used to retrieve the ambient biologically effective UV irradiances. Measurements of UV irradiance and total ozone by means of Brewer Spectrophotometry, have been started at Rome, urban site (latitude, 41.98N; longitude, 12.528E; altitude, 75 m a.s.l.) in 1992. The Rome series represents the longest available UV time series in Italy. At Saint-Christophe (Aosta), a semirural site (latitude, 45.74N; longitude, 7.36E; altitude, 570 m a.s.l.) the UV observations started in 2007. Brewer #067 is located at the Physics Department of Rome University "La Sapienza" (in the city center), while Brewer #066 is located on the roof of the building of headquarter of the Environmental Agency of Aosta Valley (ARPA Valle D'aosta) at Saint-Christophe in the Alpine region. Hereafter this station is named Aosta station.

3.1.1.1 Brewer Spectrophotometer

Both Brewers are single-monochromator instruments (version MKIV); measurements of global (direct plus diffuse) radiation are made in the spectral range from 290 to 325 nm at 0.5 nm stepwidth. The Brewer slit function is nearly triangular with a FWHM (full bandwidth at half maximum) of about 0.63nm for both instruments. Global UV irradiance spectra from 290 to 325 nm in steps of 0.5 nm were recorded every 30 min.

Systematic checks and tests (daily, weekly and monthly) are carried out to ensure a proper performance of the instruments and to guarantee the accuracy and quality of observations. Regular controls are made several times per day using internal lamps: an internal mercury lamp to assure the monochromator wavelength stability, an internal halogen lamp to check the stability of the spectrometer at the five operating wavelengths and dark-counts channel, this last one is used to estimate the background noise. According to the Guidelines for Site Control of UV Monitoring (69), at Rome the UV irradiance response is monitored routinely by using a set of 50 W calibrated lamps supplied by the Brewer Instrument manufacturer (SCI-TEC, Saskatoon, Canada) and traceable to the standards of the National Institute of Standard and Technology (NIST), Maryland, USA. The global irradiance scale of the Brewer at Aosta is calibrated monthly against a Bentham spectroradiometer (belonging to the ARPA Valle

d'Aosta) by recording synchronous spectra during several clear days (22).

The overall performance of the Brewer instruments is controlled every two years in a field calibration by the comparison with the travelling reference UV spectroradiometer QASUME (70), mantained at the PMOD/WRC (Physikalisch - Meteorologisches Observatorium Davos, World Radiation Center, (71)). The deviation in the angular response from the ideal cosine response in the Brewer #067 was determined during QASUME 's visit in 2006, showing that UV irradiances were underestimated on average by 9%. After the application of cosine and temperature correction on UV irradiances (72) (70) (73) the last comparison with QASUME spectroradiometer in 2008 showed that, the mean ratio with the travelling spectroradiometer decreased to +3% (74). The methodology for the temperature correction is described in Siani et al. (2003) (72). The spectra from the Brewer #066 are also corrected for its angular response and for temperature. The last comparison with QASUME spectroradiometer in 2011 showed an average offset and a diurnal variation of 0% and 3% respectively. The uncertainty of integrated UV irradiances is estimated at 5% for both Brewers.

3.1.1.2 SHICrivm Software Package

To improve the quality of UV spectral measurements the SHICrivm code (version 3_075) (75) was used on UV data in both sites. This

software package, developed over the past years in the context of the EDUCE (76) and SUVDAMA (Scientific UV Data Management) (77) projects, aims to improve the comparability of data sets obtained with different spectral instruments, and to insure the quality by means of checking or calibrating spectral wavelength shifts and spectral shape errors (spikes, variability).

The main functionality of the SHICrivm software are the following:

- determination of wavelength dependent spectral wavelength scale errors/shifts of the measured solar UV-spectrum by comparing the spectral structure with a high resolution extraterrestrial spectrum;
- alignment of the measured solar spectrum, correction of the wavelength error/shift;
- deconvolution of the measured spectrum;
- calculation of a spectrum corrected for wavelength shifts, and calculation of a standardized 1 nm FWHM spectrum;
- calculation of biological effective UV for a set of action spectra, and irradiances integrated over a set of wavelength intervals;
- check of the spectral structure, identifying possible (local) spectral anomalies;

- identification of the lowest irradiance levels, including the determination of the "starting" wavelength where readings become reliable;
- full-quality flagging: for wavelength shifts, for spikes and spectral shape errors, for lowest irradiance and starting wavelength of the spectrum, for (cloud) variability during the scan;
- identification of cloud-transmission and cloud variability during the scan;
- calculation of spectral atmospheric transmission;

In this study the SHICrivm code was employed to standardize the spectral UV data to 1 nm spectral resolution and to correct any small wavelength inaccuracies. The code was also applied to extend the spectral data up to 400 nm, since both Brewer Spectrophotometers measure spectral irradiance up to 325nm, and hence to calculate the photobiological quantities.

3.1.2 Ozone Data

Brewer spectrophotometers are designed to measure ground-level intensities of the attenuated solar radiation at five specific wavelengths in the Huggins absorption spectra of ozone and sulphur dioxide. The total columns of the ozone from direct sun (DS) measurements are estimated by applying the Lambert-Beer law to a

set of six wavelengths (303.2, 306.3, 310.1, 313.5, 316.8 and 320.1 nm). The first wavelength is used for spectral calibrations, the second is used for filtering the SO_2 contribution and a combination of the natural logarithm of the radiances at the four other wavelengths is used to compute the total ozone amounts in Dobson Units (DU). Every two years, the Brewers are calibrated by intercomparison with the travelling instrument #017 operated by International Ozone Services, Inc.

The total ozone amounts at Rome station started in 1992 while at Aosta station started in 2007. Total Ozone values recorded at the two stations are submitted to the WOUDC (World Ozone and Ultraviolet Data Center) (78) at the end of each year. At Rome station the O_3 data from 1992 to 2003 were processed with dedicated software: Ozorec Software and from 2004 to 2006 with O3Brewer Software. Following the WOUDC recommendations of 2008, due to some anomalous ozone values in the Rome series, a reprocessing of Rome ozone series (1992-2010) was necessary and was carried out by means of the Brewer Processing Software, BPS (ver 2.1.0, updated May 2011) taking into account only O_3 observation with standard deviation less than 2.5 DU and with air mass ≤ 3. The ozone data were also reprocessed skipping the fourth position neutral density filter which showed very high attenuation (~60% more than specification) during the calibration with the reference traveling standard #017 in 2009. First, the BPS extracts and processes the SL

(Standard Lamp) test results, then it does the ozone calculations. SL correction to ETC (Ozone Extra-Terrestrial Constant) is done using the ETCs obtained from the calibrations with the International ozone reference. The Brewer Processing Software was also employed to process total ozone data at Aosta for the period 2007 – 2010. The climatological daily total ozone amounts (hereafter called normal values) extracted from (http://es-ee.tor.ec.gc.ca/cgi-bin/totalozone) (79) were used as reference daily values. They are based on TOMS (Total ozone Monitoring Spectrophotometer) data for 1978-1988 and approximated by Fourier harmonics.

3.2 Aerosol Index from OMI Measurements

Ozone Monitoring Instrument (OMI) onboard the NASA EOS Aura space-craft, on flight from 14 July 2004, is a nadir viewing spectrometer that measures solar reflected and backscattered light in the spectral range from 270 nm to 500 nm with an average spectral resolution of 0.5 nm. The Aura satellite describes a sun-synchronous polar orbit, crossing the equator at 13:45 local time. The width of the instrument's viewing swath (consisting of 60 individual pixels) is 2600 km and it is large enough to provide global daily coverage with a spatial resolution at nadir of 13×24 km. OMI products include ozone columns, aerosol index, clouds, surface UV irradiance and trace gases (NO2, SO2, HCHO, BrO and OClO) (80).

The aerosol index is a measure of how much the wavelength dependence of backscattered UV radiation from an atmosphere (Mie scattering, Rayleigh scattering, and absorption) differs from that of a pure molecular atmosphere (pure Rayleigh scattering) (81).

The aerosol index AI is defined as:

$$AI = 100 \log10(I_{360Meas} / I_{360Calc}) \quad (3.1)$$

where $I_{360Meas}$= the measured 360 nm OMI radiance and $I_{360Calc}$= the calculated 360 nm OMI radiance for a Rayleigh atmosphere.

The AI can distinguish the contribution of absorbing and non absorbing aerosols. AI positive values are associated with UV-absorbing aerosols, mainly mineral dust, smoke and volcanic aerosols. However, negative values are associated with non-absorbing aerosols (for example, sulfate and sea-salt particles) from both natural and anthropogenic sources (82). When the value is close to zero, this indicate presence of clouds.

3.3 Photobiological quantities

Brewer instruments provide high quality measure of spectral UV irradiance ($Wm^{-2}nm^{-1}$) in the range of wavelengths 290-325nm. By means of SHICrivm code, as above described, the spectra were extended to 400 nm. The UV effectiveness in producing biological effect is ascertained by using an action spectrum S(λ) i.e a weighting

function which defines the relative effectiveness of the different wavelengths. The ambient dose rate can be determined by integrating the spectral weighted irradiance I(λ) incident on a horizontal surface over the wavelength range 290-400 nm:

$$\text{Biologically Effective Dose Rate (DR)} = \int I(\lambda)S(\lambda)d\lambda \qquad (3.2)$$

The units are in mWm^{-2} (or $W_{eff}m^{-2}$ according to several authors, where "eff" stands for "effective"). The effective dose (D) obtained by the integration of dose rate over a specified period of time (hourly, daily, weekly, monthly, yearly or other) yields the ambient dose (AD in Jm^{-2}):

$$AD = \int DR(t)dt \qquad (3.3)$$

3.3.1 Action Spectra

In this work two biological effects of solar UV exposure were considered: the erythemal effect and the photo-production of pre-vitaminD_3.

3.3.1.1 Erythemal Action Spectra

The most used action spectrum is the erythemal action spectrum, a weighting function which simulates the damage process occurring in the skin. It is used to determine the UV index (83) (84) (85). The UV index is calculated dividing a summer erythemal dose rates at mid-

day under cloud free conditions (250 mW/m^2) and so is arbitrarily divided by 25 to generate a convenient index value, which becomes essentially a scale of 0 to 10 (or more in extreme UV cases) indicating the potential sunburning of the solar radiation.

The erythemal action spectrum was proposed by McKinlay and Diffey in 1987 (26) with the aim of replacing the "Standard erythemal curves" of CIE, 1935 (86) and DIN, 1979 (87), which did not account for the UVA portion of the spectrum. In addition to information in the UVA, the "new" erythema action spectrum was based on the statistical consideration of relatively recent experimental data. In 1998 the CIE erythema action spectrum was published as a CIE standard and thereafter adopted by ISO (25).

In the course of the present study the difference existing between the 1987 and 1998 versions of the CIE erythemal action spectrum was enlightened and the CIE committee was asked to revise the erythemal action spectra. Consequently, Webb et al. (2011) (88) recently clarified that the 1998 version is the standard erythema action spectrum to be used. This spectrum (25) normalized to unity at the wavelength of maximal sensitivity (298 nm) was adopted in this study and it is shown in figure 3.1.

3.3.1.2 Vitamin D Action Spectrum

A previous version of the action spectrum for the UV-induced conversion of 7-dehydrocholesterol (7-DHC) to pre-vitamin D_3 in human skin was published in 1982 by MacLaughlin et al. (1982) (55), and indicates a maximum at about 297 nm with essentially no production above 315 nm.

In 2006 the CIE produced a standardised action spectrum for the production of previtamin D_3 in human skin taking as a starting point the McLaughlin version. The CIE action spectrum employed an algorithm for the values at 21 wavelengths between 255 and 315 nm, the intermediate points were calculated by a spline interpolation and for wavelengths below 260 nm and above 315 up to 330 nm, the action spectrum was extrapolated by exponential decay functions. It was pointed that pre-vitamin D_3 formation occurs almost entirely in the UV-B band (280–315 nm) with only about 3–4% of the total production is in the UV-A waveband.

In the present study the vitamin D_3 effective dose rates were computed using the standard action spectrum for conversion of 7-DHC to previtaminD_3 in human skin (89) normalized at 298 nm (Fig.3.1).

It ought to be noticed that the action spectrum is originates from a wavelength by wavelenght analysis, and does not take into account any spectral interaction.

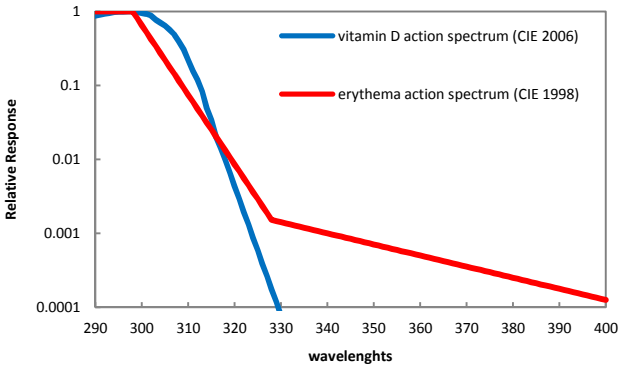

Figure 3.1 CIE erythemal action spectrum (25) and the vitamin D weighted action spectrum (89).

3.4 Climatological study design

3.4.1 Data set

The series of high quality checked spectral UV measurements allowed to determine the climatologies of erythemal and vitamin D dose rates and their ratios. The study of their variability in relation to the different geographical and environmental conditions was conducted at the two Italian sites (see paragraph 4.3 ÷ 4.8).

The erythemal (UV_{ery}) and vitamin D (UV_{vitD}) dose rates series were computed from 14 years spectra (1996-2009) at Rome and from 4 years spectra (2007-2010) at Aosta. The analyzed period at Rome was restricted to 14 years since the daily distribution of UV

observations after 1996 was more regular after 1996 providing the UV information necessary for the study. In addition, UV irradiances in 2010 was not taken into account because it was recently found that the UV responsivity used to process spectra needs a revision by a complex calibration procedure.

The first step was to retrieve UV_{vitD}, UV_{ery} and their ratio under all sky conditions at three times during the day, selected in order to mark the highest values of UV radiation (local noon, 11.00UTC), the beginning (08.00UTC) and the end (15.00UTC) of the working hours period for the majority of the population (90). UV spectra within an interval of 30 min centered on the selected times were averaged and associated to the chosen time.

Since clouds have little wavelength dependence in the 300-325 nm interval and therefore have no impact on the ratio between erythemally and vitamin D dose rate (91), only clear sky data were analyzed in detail. The clear sky days were selected taking into account only days with cloud cover less than 2/8 during the day. Those days were selected assuming a threshold value derived from the monthly average hours of sunshine climatologies. The measured daylight hours at Rome (1991-1997), were provided from the meteorological station of UCEA (Ufficio Centrale di Ecologia Agraria) at Rome and from ARPA at Aosta (1995-2010). The data were used to calculate the monthly mean values and their standard deviation. The threshold value was defined as the monthly average

sunshine hours ± 2 standard deviations for Rome and ± 1 standard deviation for Aosta. In the latter case only 1 standard deviation was considered to get a larger data set. A daily value of sunshine hours greater than or equal to the threshold value was associated to clear sky day.

The daily $UV_{vitD,}$ UV_{ery} climatologies for each site were calculated as the average of all daily UV observations from the periods under study. The ratio (UV_{vitD} /UV_{ery}) was derived and analyzed as a function of day of the year for three times during the day (see paragraph 4.6).

3.4.2 Solar Zenith Angle (SZA) calculation

The dependence of UV climatologies on the SZA corresponding to the selected times is discussed in the Results (see paragraph 4.6)

The SZA (θ_0) was calculated as follows:

$$\cos\theta_0 = \sin\delta\sin\Phi + \cos\delta\cos\Phi\cos t_h \qquad (3.4)$$

Where δ is the solar declination, i.e. the declination is the angle between the sun's direction and the earth's equatorial plane. The solar declination δ in radians is:

$$\delta = b_0 + b_1\cos\theta_n + b_2\sin\theta_n + b_3\cos 2\theta_n + b_4\sin 2\theta_n + b_5\cos 3\theta_n + b_6\sin 3\theta_n \qquad (3.5)$$

Where the coefficients b_0-b_6 are given in table 3.1.

The local hour angle t_h is the angle between the observer's meridian and the meridian of the sun. It differs from the local clock angle, thus it should first be converted to Greenwich mean time (GMT) using the appropriate time zone difference. The local hour angle (in radians) is:

$$t_h = \pi(GMT/12 - 1 + \Phi/180) + EQT \qquad (3.6)$$

where Φ is the longitude.

The last term is the equation of time (EQT), and accounts for the non uniformity of the apparent angular speed of the sun in the sky. Values of EQT may be evaluated as follows:

$$EQT = c_0 + c_1\cos\theta_n + c_2\sin\theta_n + c_3\cos 2\theta_n + c_4\sin 2\theta_n \qquad (3.7)$$

with the coefficients c_0-c_4 given in table 3.1.

The climatology of the peak UV index (at local noon) was also provided at both sites.

Taking in account the threshold value for photoconversion to previtamin D_3 ($\approx$ 3.46 mW/m^2) as proposed by Engelsen et al. (92) the behavior of the UV_{vitD} has been also studied at both sites to ascertain whether the photo-production of previtaminD_3 occurs during the year .

3.4.3 Climatological study as a function of Solar Zenith Angle (SZA)

To perform the climatological study as a function of a solar zenith angle, the UV spectral irradiances were corrected for the Sun- Earth distance variation that can be computed in terms of the day number d_n as follows:

$$(R_0/R_n)^2 = a_0 + a_1 \cos\theta_n a_2 \cos\theta_n + a_3 \cos 2\theta_n + a_4 \sin 2\theta_n \quad (3.8)$$

where R_0 is the average earth-sun distance, R_n is the earth-sun distance on day d_n, the coefficients a_0-a_4 are given in Table 3.1, and

$$\theta_n = 2\pi d_n / 365 \quad (3.9)$$

R_n varies by about 3.4% from minimum (perihelion, on about 3 January) to maximum (aphelion, on about July 5). The variation in R_n^2, and therefore in the intensity of extraterrestrial radiation, is about 6.9%, and is significant especially when considering seasonal differences in UV intensities between Southern and Northern Hemispheres.

i	a_i	b_i	c_i
0	1.000110	0.006918	0.000075
1	0.034221	-0.399912	0.001868
2	0.001280	0.070257	-0.032077
3	0.000719	-0.006758	-0.014615
4	0.000077	0.000907	-0.040849
5		-0.002697	
6		0.001480	

Table 3.1 Coefficients for Earth-Sun Distance (a_i), Solar declination (b_i) and the Equation of Time (c_i)

The UV climatologies also depend on the solar zenith angle (SZA). Three SZA values were selected for both sites: the minimum SZA reached during the year (18° at Rome and 22° at Aosta), the SZA reached from Spring to Autumn (47° in both sites), and the SZA reached during the whole year (66° at Rome and 68° at Aosta). UV spectra within an interval of 4° centered on the selected SZAs were averaged and associated to the chosen angles.

The ratio series for cloudless sky conditions and for the SZA reached during the whole year were analyzed as a function of the total ozone column. The analysis was performed for ozone values from 250 DU to 450 DU at 50 DU increments.

3.4.4 Climatological study as a function of O_3 and AI values

The behavior of the climatological ratios for cloudless sky conditions was investigated first as a function of total ozone for different values

of SZA (from 20° to 70° with 10° increments) and then as function of SZA for different values of total ozone (from 250 DU to 450 DU with 50 DU increments). Finally the influence of aerosol index on the climatological ratios was analyzed. Fixing the O_3 value of 300 DU (climatological value for mid-latitude sites), the climatological ratio were analyzed first as a function of AI for different values of SZA (from 20° to 70° with 10° increments) and then as a function of SZA for different values of AI (from -1 to 2.5 with 0.5 increments).

3.5 Radiation Amplification Factor (RAF)

The relationship between change in total column ozone (O_3) and change in biologically effective radiation (UV_{bio}) can be quantified using the Radiation Amplification Factor (RAF), defined as the percentage increase in UV_{bio} that would result from a 1% decrease in the column amount of atmospheric ozone (93). For example RAF= 1.2 implies a 1.2% increase in biologically effective irradiance for each percent decrease in O_3 amount.

For small fractional changes in ozone (of the order of 1%- 10%), the RAF for UV_{bio} can be defined as:

$$RAF = -\frac{\left(\frac{\Delta UV_{bio}}{UV_{bio}}\right)}{\left(\frac{\Delta O_3}{O_3}\right)} \qquad (3.10)$$

where ΔUV_{bio} and ΔO_3 are the changes of UV_{bio} and column ozone respectively.

For the class of action spectra that decay approximately exponentially with increasing wavelength over 300–330 nm, as the relationship between ozone and biologically effective irradiance becomes non linear with large ozone changes, an empirical power–law form can be used to describe accurately the changes in the biologically effective irradiance (UV_{bio}) due to ozone changes (94) (95) (96):

$$UV_{bio} \propto (O_3)^{-RAF} \quad (3.11)$$

The RAF is strongly wavelength-dependent, especially at shorter wavelengths where ozone absorption is large and it depends also on the solar zenith angle.

Large RAF values indicate that the radiation associated with a particular effect is strongly sensitive to changes in atmospheric ozone. Values of RAF ≈ 0 mean that the UV_{bio} for that particular effect is not dependent on ozone, as occur in cases when an action spectrum shows strong sensitivity to longer UV-A and visible wavelengths, but not to UVB radiation.

In this study the relationship 3.10 was used to calculate RAF for erythemal and previtaminD_3 effect for AI ranging from -0.5 to 0.5 (in

order to reduce the aerosol effect) and SZA ranging from 20° to 70° with increments of 10°.

3.6 Time exposure to induce erythema and for sufficient vitamin D

A recent study (29) proposed an algorithm to calculate the optimal exposure times from UV indexes (UVI) to get sufficient vitamin D without inducing the erythema. The calculation was based on the long series of UV_{ery} and UV_{vitD} at Lauder in New Zealand (29).

Using the same algorithm the exposure times for erythema and for photosynthesizing sufficient vitamin D were estimated at the two Italian sites and the results were compared with those found at the southern site.

The time needed (t_{ery} in minutes) to induce skin damage was calculated as follows (29):

$$t_{ery} = \frac{4000}{60} \frac{MEDF \cdot SPF}{UVI} \tag{3.12}$$

Where:

- 4000/60 is a factor to account for the conversions from UV_{Ery} to UVI, and seconds to minutes;

- UVI is the UV index (= 40 · UV_{Ery}, where UV_{Ery} has units of Wm^{-2});
- MEDF is a factor to account for differences in skin type (see chapter 2, session 2.1). It is expressed here as the number of SED (1 SED = 100 Jm^{-2} of UV_{Ery}) required to induce erythema.
- SPF is the sun protection factor.

The exposure time for sufficient vitamin D (t_{vitD}) was calculated taking into account the area of exposed skin expressed as percentage of total body area (A) as follows (29):

- full body corresponds to 100% (A = 1);
- face, hands, arms and legs corresponds to 63% (A = 0.63);
- face, hands and arms corresponds to 27% (A = 0.27);
- face and hands corresponds to 10% of the body area (A = 0.10).

Moreover since the recommended daily dose of vitamin D is thought to be in the range 400–1000 IU (5) (97) (98) (99) (100), it was assumed that optimal vitamin D levels are maintained by a daily intake of 1000 IU of vitamin D and that a full body exposure of pale skin under high sun conditions (UVI = 10) produces 1000 IU in less than 1 min (5) (101).

Therefore the time exposure can be estimated adopting the following conditions:

- UVI_0 = 10 (peak UV for mid-latitudes in the northern hemisphere);
- R_0 = 2 (the maximum value for R);
- t_{vitD0} = 1 min (101);
- A_0 = 1 (full body exposure);
- $MEDF_0$ = 2.5 (skin type II);
- SPF_0 = 1 (no sunscreen applied).

If the time taken to produce a specific increase in vitamin D resulting from one given set of reference conditions (0) is known, then the time t_D for any other set of conditions can be deduced by:

$$t_{vitD} = t_{vitD0} \frac{UVI_0}{UVI} \frac{R_0}{R} \frac{A_0}{A} \frac{MEDF}{MEDF_0} \frac{SPF}{SPF_0} \quad (3.13)$$

Where

- UVI is the UV index as defined above;
- R (SZA, total ozone) is the ratio of UV_{VitD} /UV_{Ery} for those conditions;
- t_D is the exposure time (in minutes);
- A is the exposed body area expressed in %;
- MEDF and SPF are as defined above.

Assuming the same skin type, body area exposed and no sunscreens, the exposure time t_D is just:

$$t_{vitD} = t_{vitD0} \frac{UVI_0}{UVI} \frac{R_0}{R} \tag{3.14}$$

3.7 Polysulphone Dosimetry study design to retrieve the pre-vitamin D dose

The most widely used UV dosimeters are polysulphone (PS) films which have a response to UV radiation similar to human skin (56) (57). Figure 3.2 shows the polysulphone action spectrum compared with the erythemal and pre-vitaminD_3 action spectra. A marked similarity, more pronounced than the erythemal case, between the spectral response of the polysulphone and the pre-vitamin D_3 action spectrum, can be noticed at shorter wavelengths. All spectra are normalized at 298 nm.

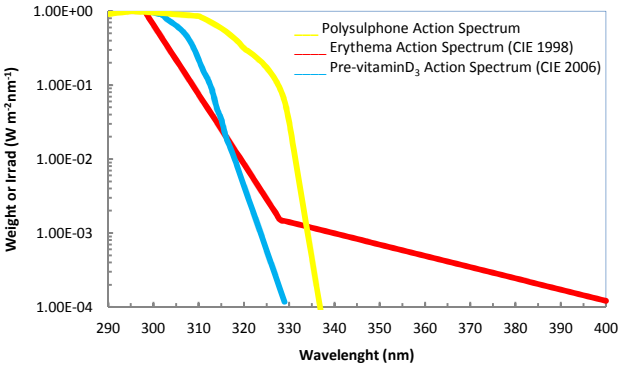

Figure 3.2 CIE erythemal (25), pre-vitamin D_3 (89) and polysulphone weighted action spectra.

The observed pattern stimulated the study of the applicability of PS dosimetry to retrieve both UV_{ery} and UV_{vitD} doses using a unique dosimeter and, hence, to simultaneously provide information on both the beneficial and damaging effects of UV exposure. Polysulphone (PS) is a polymer that, when exposed to UVR, undergoes a complex photodegradation with increased fragility. The polysulphone monomer is showed in Figure 3.3 (102).

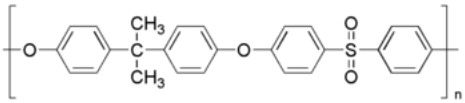

Figure 3.3 The polysulphone monomer (by courtesy of (102)).

The C-O and C-S bonds are cleaved by UV photon action. The C-S bond is more sensitive resulting in its rupture with no inverse reaction. Such degradation generates a variation of PS absorbance which can be measured to provide a measurement of the absorbed UV dose.

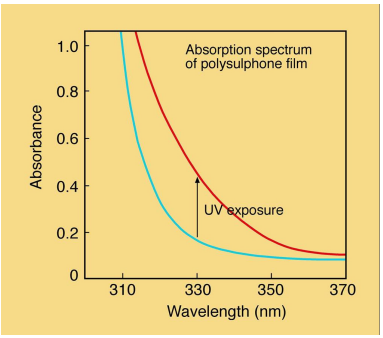

Figure 3.4 The absorption spectrum of 40 μm polysulphone film before and after exposure to UVR (by courtesy of (103)).

Figure 3.4 shows the spectral absorbance of PS before and after exposure to UV radiation. It can be noticed that 330 nm is the wavelength at which the maximum change in absorbance occurs so the absorbance change (ΔA) at 300 nm is measured and used as the response to the received UV dose.

The use of PS dosimeters requires the determination of the calibration curve i.e. a plot of ambient dose D versus change in PS film absorbance ΔA, before and after exposure, for each dosimetric experiment.

The calibration curve is obtained by exposing a set of PS dosimeters on horizontal plane at specific time intervals and simultaneously measuring the ambient UV dose using a calibrated instrument (radiometer or spectroradiometer). Dosimeters exposed on a flat horizontal plane near the radiometer have the same 2π field of view of the radiometer. The dose-response relation can be represented by a fitted third-degree polynomial and it is usually parameterized by a coefficient (c) multiplying a cubic polynomial function (104) (105):

$$D = c\,(\Delta A + \Delta A^2 + 9\Delta A^3) \qquad (3.15)$$

where D is expressed either in J m^{-2} or kJ m^{-2} and the coefficients of ΔA reflect the intrinsic characteristic of the polysulphone photodegradation reaction. The mismatch between the polysulphone action spectrum and the biological action spectrum causes the

dependence of the polysulphone absorbance on the UV radiation exposure and is responsible for the variability of the polysulphone calibration curves. A recent study (106), demonstrated that the variability of the coefficient c could be attributed to the different environmental conditions during each field campaign, mainly to the total atmospheric ozone amount and the solar zenith angle. This implies that calibration curves valid for all environmental conditions do not exist and the calibration should be obtained for each dosimetric campaign.

Following the definition of g given by (107) and according to (106), there is proportionality between c and the parameter g for the erythemal case:

$$g_{ery} = 1000 \cdot c_{ery} \cdot \alpha \qquad (3.16)$$

where α is a constant equal to 7.4·10-5 m^2J^{-1} and g_{ery} is the ratio between the erythemal dose rate and the polysulphone dose rate calculated as follows:

$$g_{ery} = \frac{\int I(\lambda)S^{E}(\lambda)d\lambda}{\int I(\lambda)S^{PS}(\lambda)d\lambda} \qquad (3.17)$$

where I(λ) is the solar spectral irradiance at the Earth's surface, $S^E(\lambda)$ is the spectral response for the erythemal effect and $S^{PS}(\lambda)$ is the spectral response of the polysulphone film.

Similar analytical relationships can be assumed for the determination of the calibration curve for pre-vitamin D_3 dose. At first, α reported in equation (3.18) is also used as a proportionality coefficient between g_{vitD} and c_{vitD}:

$$g_{vitD} = 1000 \cdot c_{vitD} \cdot \alpha \tag{3.18}$$

This is justified by the fact that the dosimeters used for erythemal and vitamin D calibration curves have the same thickness (40 μm) and the two action spectra are quite similar.

Using the same approach of (3.17), g_{vitD} can be defined as:

$$g_{vitD} = \frac{\int I(\lambda) S^{D}(\lambda) d\lambda}{\int I(\lambda) S^{PS}(\lambda) d\lambda} \tag{3.19}$$

where $S^{D}(\lambda)$ is the action spectrum for the synthesis of pre-vitamin D_3. A link between g_{vitD} and g_{ery} can be found by multiplying and dividing (3.19) by the erythemal dose rate. It can be easily seen that g_{vitD} can thus be expressed as a function of g_{ery} and the ratio between UV irradiances weighted with the pre-vitamin D_3 and the erythemal action spectra:

$$g_{vitD} = \frac{\int I(\lambda) S^{D}(\lambda) d\lambda}{\int I(\lambda) S^{PS}(\lambda) d\lambda} = \frac{\int I(\lambda) S^{D}(\lambda) d\lambda}{\int I(\lambda) S^{E}(\lambda) d\lambda} \cdot \frac{\int I(\lambda) S^{E}(\lambda) d\lambda}{\int I(\lambda) S^{PS}(\lambda) d\lambda} = \frac{UV_{vitD}}{UV_{ery}} \cdot g_{ery} \tag{3.20}$$

The relationship between the coefficients of the erythemal calibration curves (c_{ery}) and the vitamin D calibration curves (c_{vitD}) can be found dividing by (1000 · α) the first and the last member of the equation (3.20), obtaining:

$$c_{vitD} = \frac{UV_{vitD}}{UV_{ery}} \cdot c_{ery} \tag{3.21}$$

where the ratio in this study was derived by the time series of UV_{ery} and UV_{vitD}.

3.7.1 Study Protocol

Data collected during seven PS field campaigns performed in 2004-2006 were used together with additional three field campaigns in 2010-2011, carried out to validate the proposed methodology. All calibrations were performed at Rome, where Brewer UV spectral data were available.

The polysulphone film dosimeters were manufactured by the Southern Queensland University, Australia, with a thickness of 40 mm. For each campaign a series of 20 dosimeters were exposed on horizontal plane to solar UV radiation and removed at specific time intervals, chosen by the operator. Simultaneously the corresponding dose was measured by the Brewer spectrophotometer. Absorbance, before and after exposure to solar UV radiation, was measured in the

laboratory by using a standard UV spectrophotometer (Perkin Elmer Lambda 5 UV-Vis double beam Spectrometer). More details on the spectrometer can be found in Casale et al. (2006) (106).

The ambient UV doses versus corresponding absorbance changes, measured by the Brewer, were fitted with the cubic polynomial function (3.15) providing the calibration curves for both erythemal and vitamin D effects. Values of c_{ery_bre} and c_{vitD_bre} values were determined for each campaign under study using a least squares regression method. The uncertainty associated with doses, estimated by equation (3.15), depends on random errors, because systematic uncertainties are removed when dosimeters which have the same thickness and belong to the same batch (56), as is our case. The uncertainty on D was estimated to be ±10% as derived from the error propagation formula taking into account an uncertainty of 0.001 on ΔA (56).

Reference values of c_{ery_mod} and c_{vitD_mod} were determined by means of equations 3.16 – 3.21 using measured spectral data. Two look-up tables were obtained, for the erythemal and vitamin D calibrations, for ozone values ranging from 250 DU to 450 DU at steps of 50 DU and for SZA ranging from 20° to 70° at steps of 10°. A reference table similar to c_{ery_mod} table, but based on a radiative transfer model, had already been obtained by Casale et al. (2006) (106). A comparison between c reference values and c experimental values obtained for each experiment was performed.

4 Results

4.1 Ground based UV and ozone measurements

4.1.1 Ozone Data

The total ozone (O_3) series measured by the Brewer spectrophotometer at Rome station (1992-2010) and at Aosta station (2007-2010) are shown in Fig. 4.1 and 4.2 respectively. In both figures ± 2 standard deviation (±2 std) with respect to the climatological daily total ozone amounts (hereafter called normal values (O_{3norm}), see chapter 3, paragraph 3.1.2) used as reference values, are plotted. The long term ozone daily means at Rome derived by O_3 series are plotted in Fig 4.3. The bias ((O_{3norm} – O_3 daily means)*100/ O_3 daily means)) is 2.3%.

The first two figures show the expected seasonal variation (108) with maximum values in spring and minimum values in fall as better highlighted by figure 4.3.

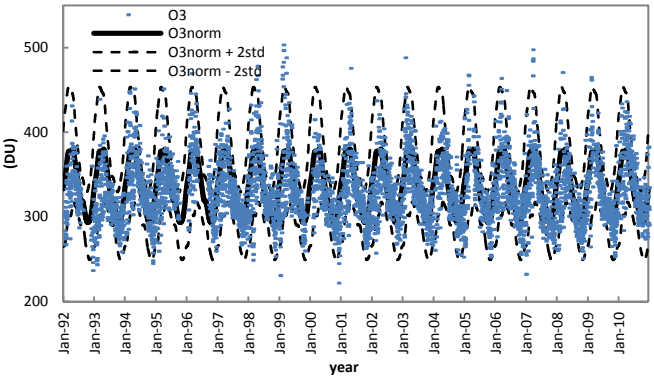

Figure 4.1 Daily total ozone (O_3) at Rome for the period 1992-2010 measured by Brewer spectrophotometer #067.

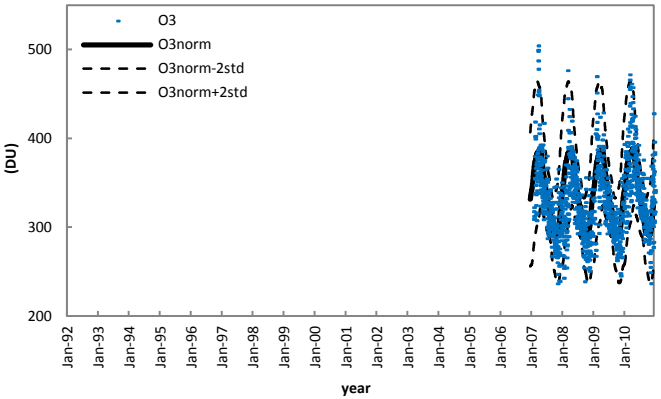

Figure 4.2 Daily total ozone values (O_3) at Aosta for the period 2007-2010 measured by Brewer spectrophotometer #066.

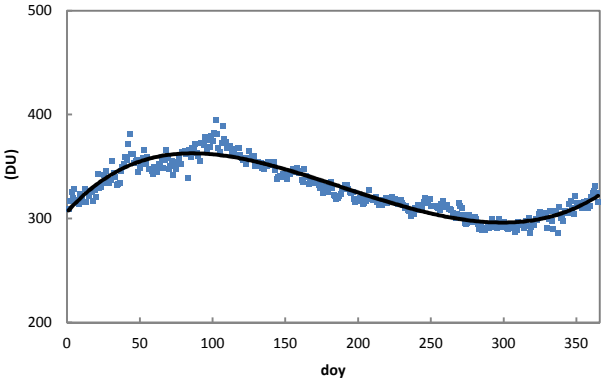

Figure 4.3 Long term ozone daily means derived by O_3 series at Rome measured by Brewer spectrophotometer #067. The solid line indicate the smoothed fit of data.

The following table summarizes the annual and seasonal ozone means.

	Total ozone (DU)				
	Annual mean ±std	**Winter mean ±std**	**Spring mean ±std**	**Summer mean ±std**	**Autumn mean ±std**
Rome	329.0 ± 8.0	332.7 ± 14.4	351.5 ± 15.4	323.5 ± 8.5	304.7 ± 8.1
Aosta	329.8 ± 11.6	331.9 ± 19.1	369.8 ± 12.9	322.1 ± 8.6	294.6 ± 7.7

Table 4.1 Annual and seasonal total ozone amounts at Rome and Aosta.

The absolute maximum and minimum values recorded at Rome station were 503.3 DU (14 February 1999) and 221.8 DU (29 November 2000), respectively, while at Aosta were 504.0 DU (24 March 2007) and 236.2 DU (8 November 2007).

Climatological ozone annual values were computed by averaging daily values for each year. Figure 4.4 shows the yearly O_3 means at Rome (the symbol indicates the measured data) and the yearly zonal ozone means (O_{3zonal}, solid line) (109) derived from ground based instruments at latitudes between 30°N-60° N. It can be noticed that the zonal O_{3zonal} means show a slowing negative trend from the 1970s to 1990s followed by a gradual recovery of ozone. This may be associated to the success of the Montreal Protocol in reducing the ozone depleting substances (61). The year-to-year Rome O_3 variability is in agreement with the zonal behavior. The low values at the beginning of the 90s can be attributed to the Pinatubo volcano eruption in 1991 (110).

In this work the Italian O_3 series were used to analyze the influence of total ozone on both biologically effective UV irradiances variability at the two Italian sites.

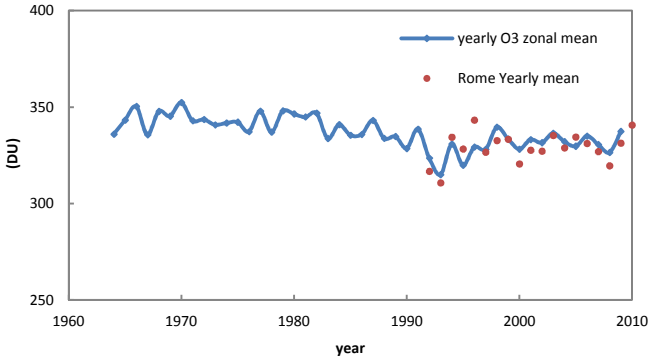

Figure 4.4 Yearly zonal ozone (O_{3zonal}) means (30°-60° N) and yearly O_3 means at Rome.

4.1.2 Aerosol Index

Aerosol Index (AI) values used in this analysis cover the period 2004-2009 at Rome site and 2007-2010 at Aosta. Figure 4.5 shows the daily AI series at Rome ranging from the maximum value of 2.9 to the minimum of -2.1. The number of observations for AI > 0 is 1306 while for AI < 0 is 476.

Figure 4.6 shows the daily AI series at Aosta, ranging from the maximum of 4.9 to the minimum of -1.82. The number of observations for AI > 0 is 613 while for AI < 0 the number of observations is 686 (see paragraph 3.2).

Since Aosta is a semirural site, negative AI values (non-absorbing aerosols, AI_{Nabs}) are prevailing compared to the

urban site of Rome where positive AI values (absorbing aerosols, AI_{abs}) are experienced.

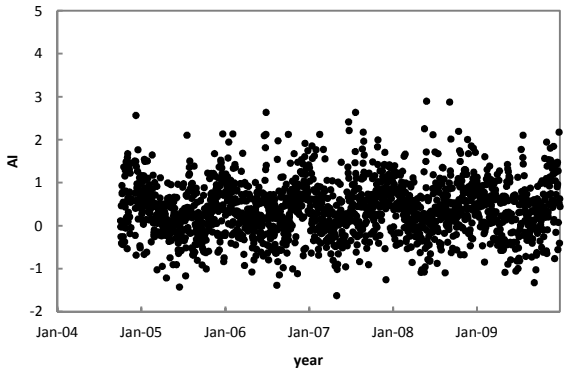

Figure 4.5 Time series (2004-2009) of daily means Aerosol Index at Rome.

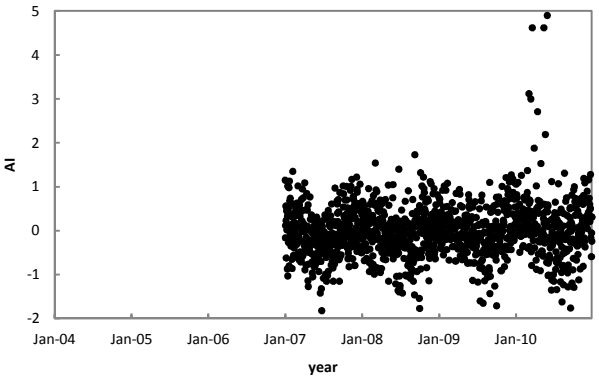

Figure 4.6 Time series (2007-2010) of daily means Aerosol Index at Aosta

Tables 4.2 and 4.3 summarize the annual and seasonal AI (absorbing and non absorbing) means.

	Rome				
	Annual	**Winter**	**Spring**	**Summer**	**Fall**
AI_{abs}	0.69±0.10	0.81±0.07	0.50±0.10	0.61±0.09	0.70±0.11
AI_{Nabs}	- 0.36±0.04	-0.35±0.07	-0.35±0.06	-0.41±0.07	-0.33±0.07

Table 4.2 Annual and seasonal AI (absorbing and non absorbing) means at Rome.

	Aosta				
	Annual	**Winter**	**Spring**	**Summer**	**Winter**
AI_{abs}	0.45±0.09	0.45±0.06	0.50±0.22	0.34±0.03	0.47±0.02
AI_{Nabs}	-0.43±0.03	-0.30±0.09	-0.38±0.27	-0.52±0.04	-0.46±0.07

Table 4.3 Annual and seasonal AI (absorbing and non absorbing) means at Aosta.

4.1.3 Solar Zenith Angle

Most of variability of UV radiation during the year is attributed to the solar zenith angle (SZA). At low solar zenith angles, photons must travel longer distances through the ozone layer, increasing the probability of absorption. The enhanced probability of interaction with air molecules leads to absorption or backscattering into space thus attenuating UV radiation at surface.

Figures 4.7 and 4.8 show the different variability of SZA through the year at the three selected times at Rome and Aosta, respectively, which can affect the measured daily dose rates at the two sites in different ways.

The solar zenith angle during local noon is less than 66° at Rome and 68° at Aosta through the year. The largest values are reached during the winter while the lowest during the summer.

The lowest value is 18°.6 at Rome and about 22.3° at Aosta, while the highest is about 85° at both sites. The figures also show as SZA behavior at the local noon is similar for both sites. On the other hand differences can be noticed on the behavior of the SZA at 08 and 15 UTC between the two sites. At Rome the SZA values at 08 UTC are always smaller than those at 15 UTC, while at Aosta the SZA at 08 UTC is higher than that at 15 UTC until around the day 100 and for the days 175-225 and lower around the day 125-175 and 250-365.

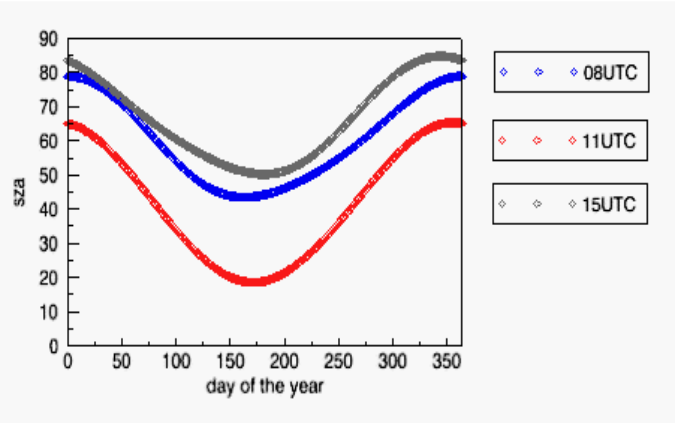

Figure 4.7 SZA at Rome

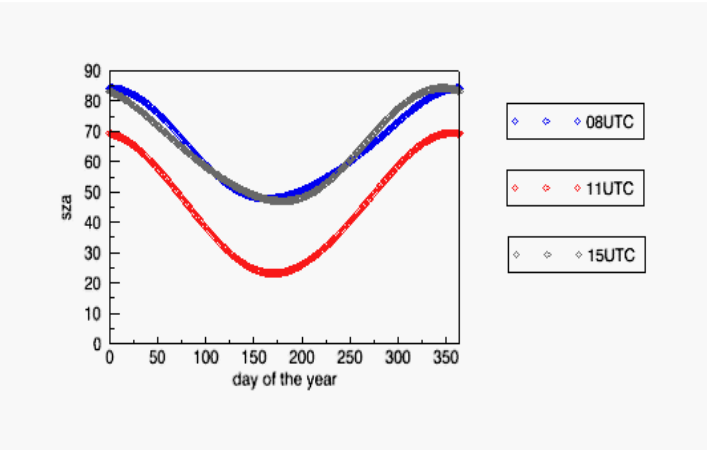

Figure 4.8 SZA at Aosta

4.2 Long term changes in erythemal dose rate

Examination of climatological series of monthly ozone values (Fig 4.9) and erythemal dose rates in terms of UV index at local noon at Rome (Fig 4.10) did not show any linear trend, probably because the time series is still too short (14 years) to detect a reliable trend. In addition to the total ozone, cloudiness and pollutants can mask the detection of possible long term UV changes.

Looking only at the clear sky summertime peak UV Index (June - July - August for the summers of 1996 – through 2009) and corresponding measured total ozone (Fig. 4.11) a moderate inverse correlation (r = -0.66) can be observed.

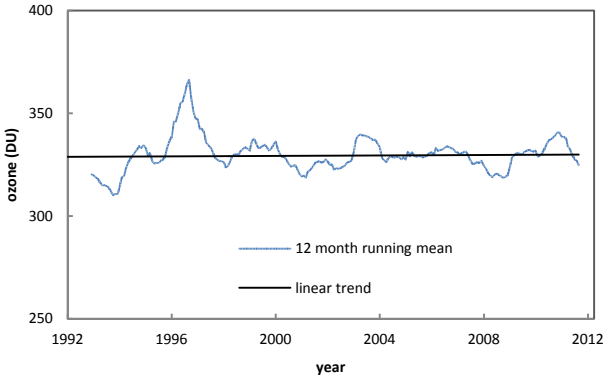

Figure 4.9 Total ozone over the period 1992-2010 (blue line is 12 month running mean, black line is linear trend)

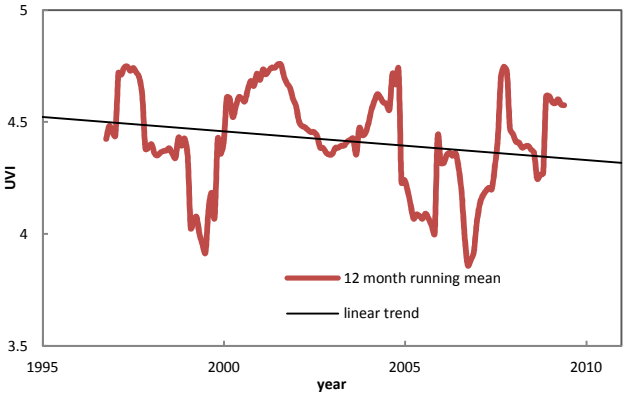

Figure 4.10 UV index at local noon (red line is 12 month running mean, black line indicates the linear trend)

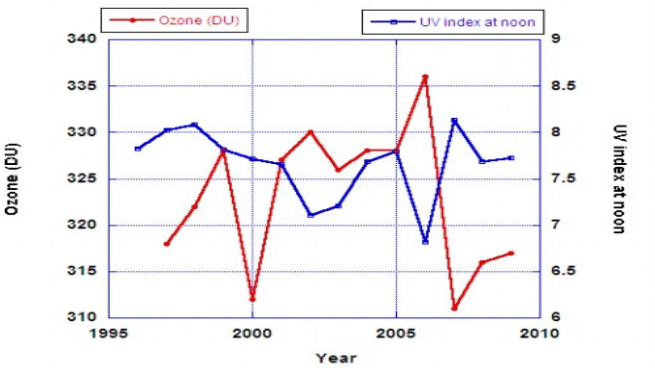

Figure 4.11 Summertime UV and ozone at Rome

4.3 Seasonal and diurnal variability of ambient biologically effective UV irradiance

The extinction of extraterrestrial solar UV radiation depends on the atmospheric scattering and absorption processes: the greater the amount of absorbing and scattering material encountered by radiation on its path, the smaller the amount of radiation reaching the surface. Figure 4.12 shows a typical global solar UV irradiance spectra (290-400nm) at the Earth surface. The spectral irradiances were measured at Rome at local noon on cloudless days close to the summer and winter solstices with comparable total ozone amounts (O_3= 317 DU in winter and O_3= 325 DU in summer). All the curves are plotted on a logarithmic vertical scale.

The difference between the two solar spectra is mainly due to different SZAs at local noon, larger solar zenith angle (SZA = 66.7°) in winter than in summer (SZA = 18.6°). The figure shows as the irradiance decreases at wavelengths shorter than 300 nm, attributable to the strong absorption by atmospheric ozone. The figure also includes the weighting functions for erythema (25) and for pre-vitamin D_3 production (111) used in this study, each of these is normalized to unity at the wavelength of 298 nm corresponding to their maximum values.

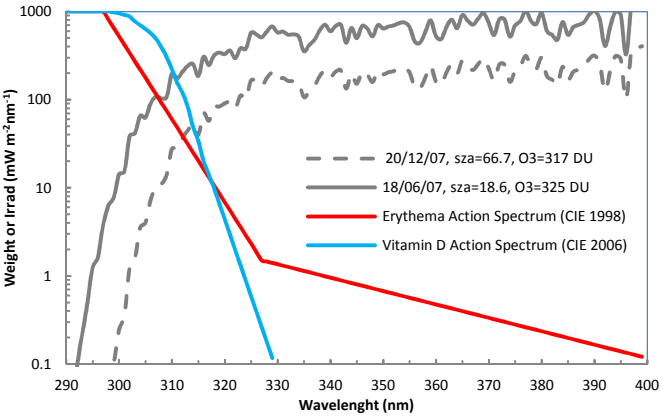

Figure 4.12 Semi-log plot of erythema and pre-vitamin D_3 synthesis action spectrum together with a typical clear sky UV spectrum measured at Rome at local noon time, near the summer and winter solstices. Both spectra and total ozone are measured by a Brewer spectrophotometer #067.

For shorter wavelengths (below 300 nm), the weighting coefficients of the two action spectra are similar. Between 300

and 325 nm both erythemal and vitamin D action spectra are particularly sensitive and the difference between the two action spectra is particularly remarkable. Above 325 nm there are only contribution of erythemal weights. For the above days the weighted spectral irradiance for erythema (UV_{Ery}) and vitamin D (UV_{VitD}) effect are plotted in Fig. 4.13 to show the large seasonal changes which are indeed in contrast with the long term UV trend. In the figure only the wavelength region from 290 to 330 nm is shown because the contribution from UV-A is small, especially in the case of vitamin D - weighted UV. Most of the seasonal variability is due to the SZA and Earth-Sun distance. The latter varies about 3.4% from minimum (perihelion, on about Jan 3rd) to maximum (aphelion, on about July 4th). The lower SZA is experienced in summer. In this case the shorter wavelengths dominate and the contribution in UVB region of the pre-vitamin D_3 weights is larger than that of the erythemal-weights. This behavior is more remarkable in summer than in winter.

The integration of weighted irradiances over the UV wavelengths yields 220 mWm^{-2} for erythema and 440 mWm^{-2} for pre-vitamin D_3 in summer; in winter is 29 mWm^{-2} for erythema and 40 mWm^{-2} for pre-vitamin D_3.

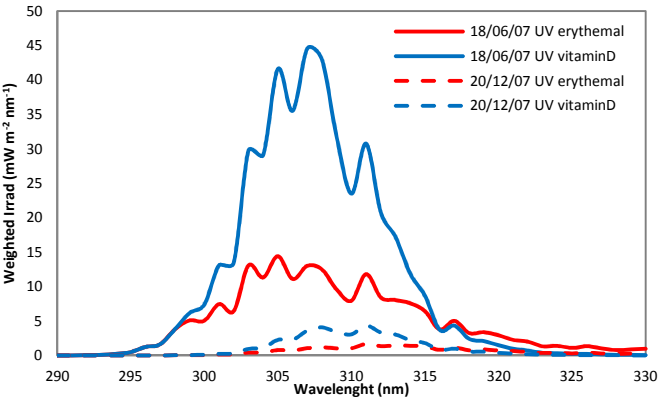

Figure 4.13 Spectral erythema and pre-vitamin D weighted irradiances close to the summer (18/06/2007) and winter (20/12/2007) solstices.

The diurnal behavior of these quantities is shown in Fig. 4.14. It can be noticed that in summer vitamin D weighted UV is larger than erythemal dose rate for the whole day, and the variation is more remarkable around local noon.

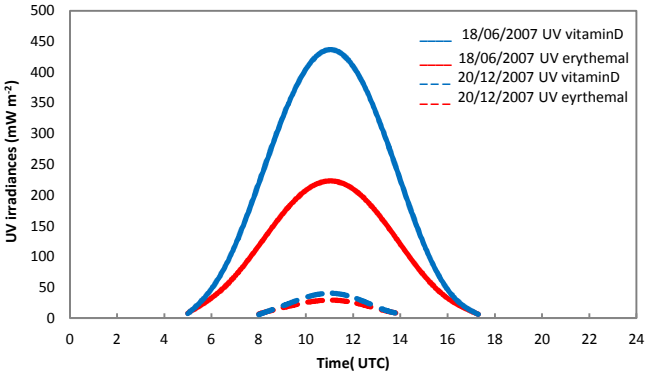

Figure 4.14 Diurnal variations in weighted irradiances on a clear day near the solstice period at Rome in 2007

The noon values of Vitamin D dose rate in winter are about 5% of those in summer while the winter erythemal values are about 10% of those in summer. This seasonal behavior results consistent with those observed at a southern mid latitude site (45°S) (29).

4.4 Climatology of the biologically effective UV dose rate at 08, 11 and 15 UTC

Climatology discussed in this study are based on 103856 spectra (all sky conditions) in Rome over the period 1996-2009 and 55726 (all sky conditions) spectra over the period 2007 -2010 in Aosta. Over the periods under study 32% of days at Rome are related to clear sky conditions and 15% cloud free days are experienced at Aosta. UV_{vitD} and UV_{ery} dose rate time series (at 08, 11 and 15 UTC (Universal Time Clock)) at the two sites were inferred in all sky conditions and clear sky conditions. Table 4.3 reports the UV_{ery}, UV_{vitD} peaks (Max), the lowest values (Min) and mean values with standard deviation for UV_{ery}, UV_{vitD} at the two sites under all sky (as) and clear sky (cs) conditions. Peak values of UV_{ery}, UV_{vitD} are experienced during the summer at local noon. At Rome they are respectively: 251.2 mW/m^2 and 480.4 mW/m^2 and at Aosta they are 232.5 mW/m^2 and 453.1 mW/m^2. The minimum

values are respectively: 0.20 mW/m^2 at 08 UTC and 0.10 mW/m^2 at 15 UTC at Rome , 0.10 mW/m^2 and 0.04 mW/m^2, during the winter at 08 UTC at Aosta.

Rome							
Sky Conditions		**UTC**	**N° days**	**Min**	**Max**	**Mean Value**	**std**
AS	**UV_{ery}**	**08**	3929	0.2	141.2	45.2	34.6
		11	4049	0.3	251.2	95.8	64.7
		15	2625	0.2	86.1	37.7	23.0
	UV_{vitD}	**08**	3929	0.1	239.1	73.4	62.8
		11	4049	0.2	480.4	173.9	127.8
		15	2625	0.1	149.2	57.1	39.52
CS	**UV_{ery}**	**08**	1279	1.1	141.2	57.6	36.0
		11	1316	7.7	251.2	123.5	61.0
		15	923	1.5	86.1	47.9	23.4
	UV_{vitD}	**08**	1279	1.0	239.1	95.5	63.9
		11	1316	8.2	480.4	226.8	123.2
		15	923	1.0	149.2	74.1	40.7
Aosta							
Sky Conditions		**UTC**	**N° days**	**Min**	**Max**	**Mean Value**	**std**
AS	**UV_{ery}**	**08**	1146	0.1	108.7	32.6	28.9
		11	1148	0.7	232.5	87.5	62.3
		15	1147	0.2	96.1	28.5	26.2
	UV_{vitD}	**08**	1146	0.1	204.6	50.8	50.8
		11	1148	0.8	453.1	157.8	124.1
		15	1147	0.1	171.0	43.6	45.9
CS	**UV_{ery}**	**08**	165	2.8	108.7	43.2	28.8
		11	170	18.3	232.5	118.3	59.3
		15	164	1.8	96.1	41.2	28.3
	UV_{vitD}	**08**	165	1.5	204.6	67.46	52.0
		11	170	19.1	453.1	214.3	121.1
		15	164	0.9	171.0	63.6	51.7

Table 4.4 Peak (Max), minimum (min), mean value and its standard deviation of the biological effective UV dose rate series at Rome and Aosta station. The units are mW/m^2.

Figures 4.15, 4.16, 4.17, 4.18 show the day to day variability throughout the year of UV_{vitD} and UV_{ery} at the selected three times.

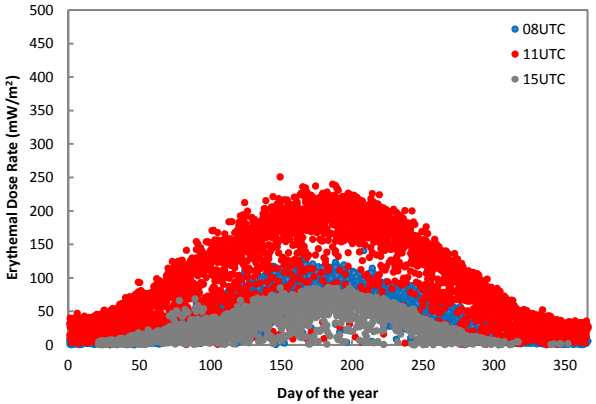

Figure 4.15 Erythemal (UV_{ery}) dose rate at 08, 11 and 15 UTC throughout the year at Rome in all sky conditions.

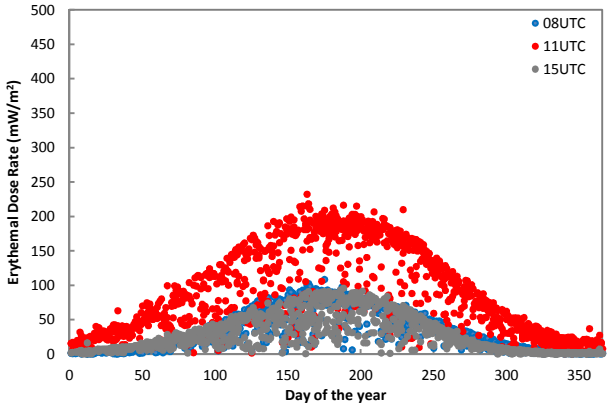

Figure 4.16 Erythemal (UVery) dose rate at 08, 11 and 15 UTC throughout the year at Aosta in all sky conditions.

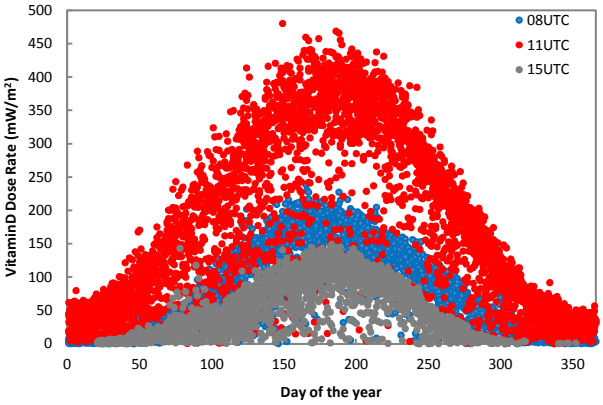

Figure 4.17 Vitamin D (UVvitD) dose rate at 08, 11 and 15 UTC throughout the year at Rome in all sky conditions.

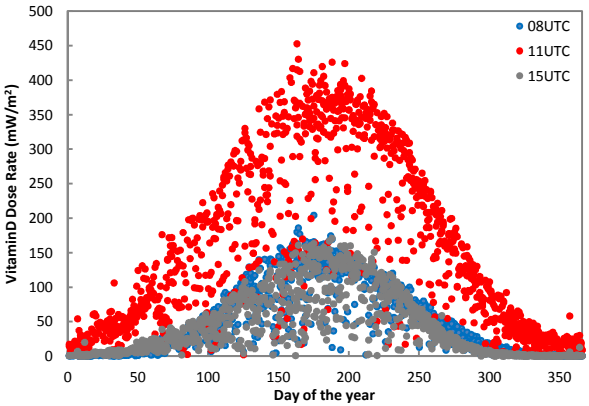

Figure 4.18 Vitamin D (UVvitD) dose rate at 08, 11 and 15 UTC at Aosta in all sky conditions.

The upper envelops of the plotted series at the selected three times can be considered as representative to cloud free conditions.

A typical behaviour is observed at both sites, with highest values in the summer and lowest in the winter due to the combination effect of lower total ozone and SZA in July. Comparing the behavior at the three selected times the maximum values are always observed at local noon (11 UTC) as expected due to the dominant effects of solar zenith angle. The figures also show as UV_{vitD} is always higher than UV_{ery} at both sites, even if, as expected, the difference is more remarkable during the summer.

Based on the clear sky UV series, the climatology of UV Index at local noon (erythemal dose rates divided by $25 mWm^2$ (112)) is provided at Rome and Aosta (fig 4.21 and 4.22 respectively). The UV Index distribution was divided into five classes for average photosensitivity as shown in figure 4.19 (112): low (0–2), moderate (3–5), high (6-7), very high (8-10) and extreme (>11). Each class is characterised by a different colour: green (low), yellow (moderate), orange (high), red (very high) and extreme (violet). Below the threshold value of 3 (112) the radiation damage for very sensitive fair skinned people (phototype I and II) is limited and no protection

measure is required. Above that value protective measures are necessary (figure 4.19 reports the recommended sun protection scheme). Figure 4.20 shows the frequency distributions for each category.

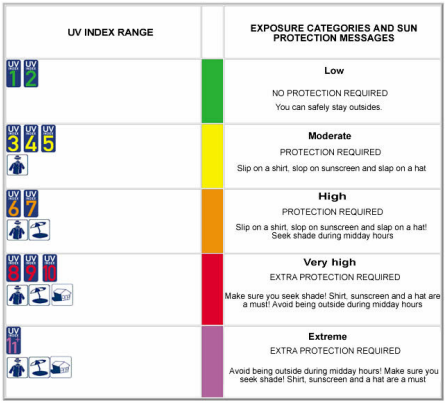

Figure 4.19 UV radiation exposure categories and recommended sun protection scheme, by courtesy of (36).

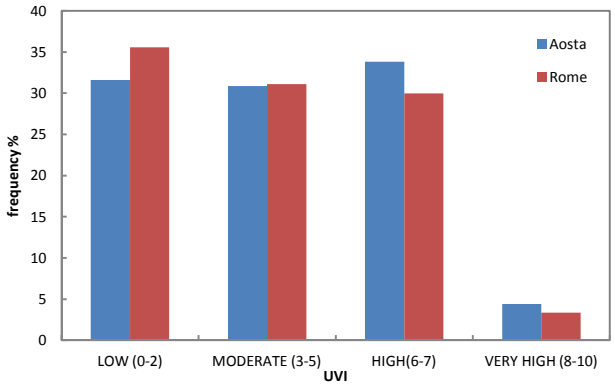

Figure 4.20 The frequency distributions for each category of UV index at Rome and Aosta.

Figures 4.21 and 4.22 show that very high values (above 8) are experienced in both sites. It can be noticed that high (6<UVI<7) classes is experienced in Summer: 30% of cases at Rome and 33.8% of cases at Aosta. On the contrary about 3.4% and 4.1% of cases are included in the Very High category for both sites.

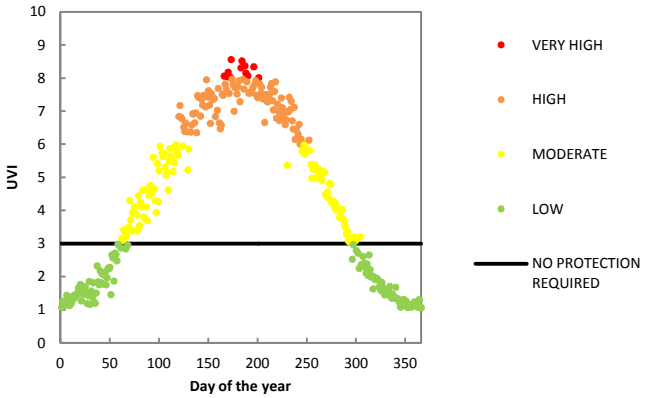

Figure 4.21 Climatology of UV Index (UVI) at local noon at Rome. Black line indicates that protection is required above that level.

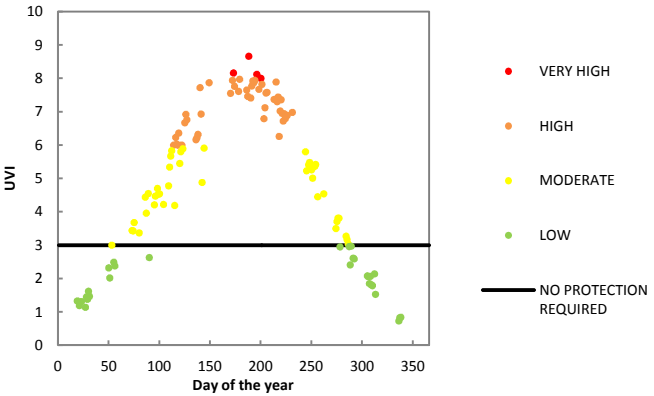

Figure 4.22 Climatology of UV Index (UVI) at local noon at Aosta. Black line indicates that protection is required above that level.

Engelsen et al. (92) proposed a detection threshold value for photoconversion to previtamin D of 3.46 mW/m^2 which is plotted as solid line in Figures 4.23, 4.24. The uppermost envelops of the three times patterns correspond approximately to cloud free conditions.

We found that at the two Italian sites the exposure at local noon allows photo-production of pre-vitaminD_3 throughout the year. However some large dose rate decreases can be experienced at local noon from October to April, attributed to strong cloud effects. Consequently Vitamin D photo-production cannot be sustained in these cases. The Vitamin D dose rates are below the threshold value from mid – November to the end of January at Rome at 15 UTC and for the same

period at Aosta at 08 and 15 UTC. This means that UV irradiance is weak for the vitamin D photoproduction. These results are in accordance with those found at the mid-latitude site of Thessaloniki, Greece (40.63°N 22.95°) (92).

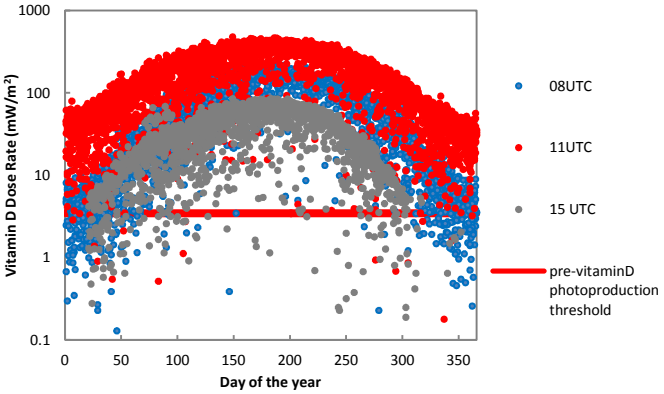

Figure 4.23 Vitamin D (UV_{vitD}) dose rate at three hours during the day and the proposed detection threshold value (92) for photo conversion to pre-vitamin D at Rome in all sky conditions

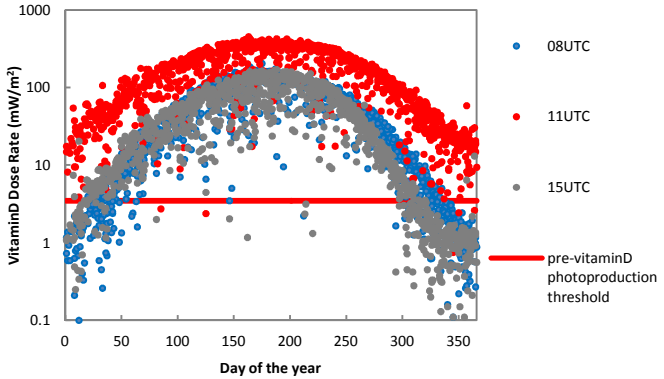

Figure 4.24 The UV_{vitD} dose rate at three hours during the day and the proposed detection threshold value (92) for photo conversion to previtamin D at Aosta in all sky conditions

4.5 Relationship between vitamin D and erythemal dose rates

Figures 4.25 and 4.26 show vitamin D rate versus erythemal dose rate at both sites under all sky conditions. Under clear sky conditions the patters are similar (not shown). Looking at both figures a linear relationship seems to well fit the data: the pre-vitamin D_3 dose rate is about twice the erythemally dose rate. Kazantzidis et al. 2009 (90) proposed that the non linear relationship between the two photobiological quantities can be better represented by a fitted polynomial of second degree than a linear fit. Their explanation is that the vitamin D action spectrum is more sensitive to solar irradiance at lower UV-B wavelengths. We obviously agree with the last statement, and in what follows the dependence on SZA and ozone is examined in such context.

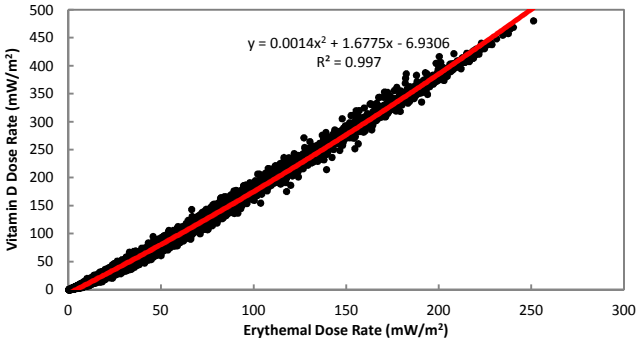

Figure 4.25 Vitamin D effective dose rate as a function of erythemal dose rate for Rome. Thick solid line represents a polynomial fit of second degree according to (86).

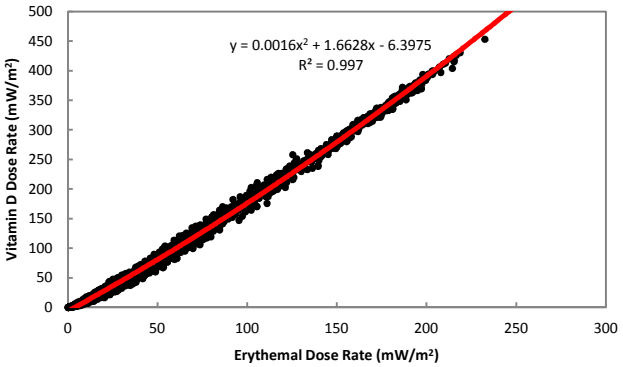

Figure 4.26 Vitamin D effective dose rate as a function of erythemal dose rate for Aosta. Thick solid line represents a polynomial fit of second degree according to (86).

4.6 Yearly variability of the ratio (UV_{vitD} /UV_{ery}) as a function of SZA and of total ozone

Figures 4.27 and 4.28 show the daily ratios (UV_{vitD}/UV_{ery}) at the two sites for cloud free days. It can be noticed that at midday the pre-vitamin D_3 dose rate is twice the erythemally dose rates in summer, while in winter the ratio is less than 1.0 at 8 and 15 UTC . In Winter the increased optical path of solar irradiance through the atmosphere (i.e higher solar zenith angles) and the enhanced scattering can lead to a much stronger reduction of UV_{vitD} compared with UV_{ery}, due to the larger sensitivity of the pre-vitamin D_3 action spectrum in the UVB region. In this case the erythemal effect can prevail.

This result is consistent with those found at European sites (12) and at Lauder (45°S) in New Zealand (29).

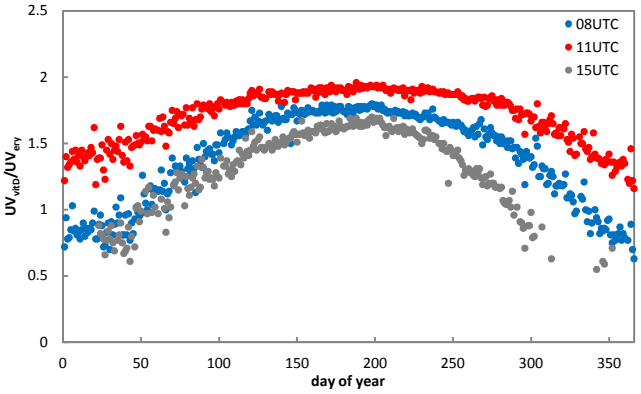

6

Figure 4.27 Climatological daily ratio (UV_{vitD}/UV_{ery}) over 14 years of measurements at Rome as a function of the day of the year.

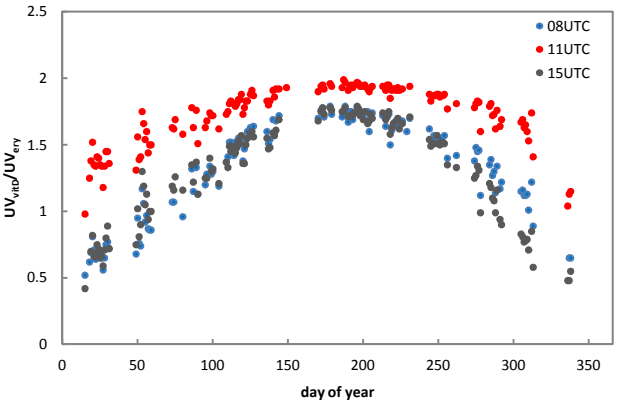

Figure 4.28 Climatological daily ratio (UV_{vitD}/UV_{ery}) over 4 years of measurements at Aosta as a function of the day of the year.

Figures 4.29, 4.30 show the impact of SZA on the ratio throughout the year at the three SZAs taken into account (20°, 47°, 66° at Rome; 24°, 47°, 68 at Aosta, see paragraphs 3.4.3).

The ratio is about 2 around noon when the sun is high (low SZA) and decreases to below 1.5 for higher SZA in winter. It can be noticed that the annual behavior of the ratios for higher SZA include the seasonal ozone cycle. The spring ozone columns are higher than the summer values, leading to a slight decrease in the ratio (mainly shown at Rome). This arises because the UV_{vitD} irradiance weights the short wavelengths more heavily than the longer wavelengths.

By comparing the three curves the annual ratio shows much less variation compared to the ratio variation as a function of the solar elevation and the annual ozone cycle has a small influence compared with this factor.

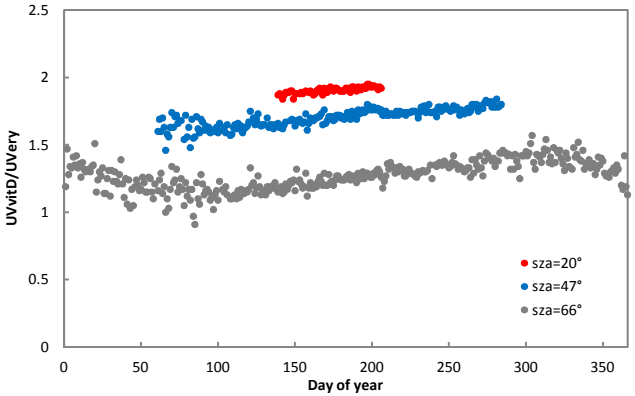

Figure 4.29 Climatological average daily ratio (UV_{vitD}/UV_{ery}) over 14 years of measurements at Rome as a function of the solar zenith angle.

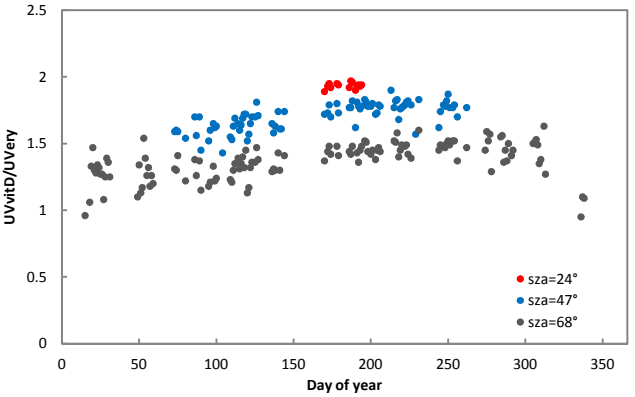

Figure 4.30 Climatological average daily ratio (UV_{vitD}/UV_{ery}) over 4 years of measurements at Aosta as a function of the solar zenith angle.

When the ratios were analyzed by fixing total ozone amount, their variability (the ratio ranges on average between 1.5 and 1) is smaller compared with those related to SZAs (Figures 4.31 and 4.32). The ratio becomes less than the unity for higher ozone (450 DU). This is still due to the more sensitive of the pre-vitamin D_3 action spectra to the UVB wavelengths.

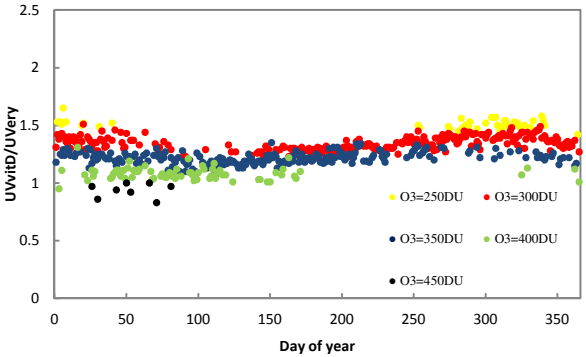

Figure 4.31 Climatological averages of daily ratio (UV_{vitD}/UV_{ery}) over 14 years of measurements at Rome as a function of total ozone values.

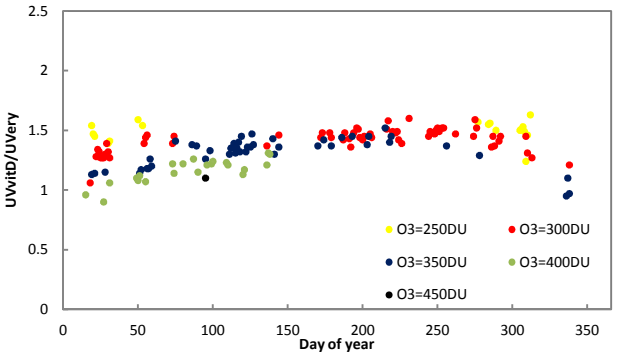

Figure 4.32 Climatological average daily ratio (UV_{vitD}/UV_{ery}) over 4 years of measurements at Aosta as a function of total ozone values.

4.7 Climatological Ratios (UV_{vitD}/UV_{ery}) as a function of SZA and total ozone

In this paragraph the behavior of the climatological ratio is examined in more detail, first as a function of total ozone for different SZAs (from 20° to 70° with 10° increments) and then as a function of SZA for different total ozone amounts (from 250 DU to 450 DU with 50 DU increments). The behaviors are presented in Figures 4.33, 4.34, 4.35, 4.36.

Figures 4.33 and 4.34 appear as a collection of nearly straight lines suggesting that the ratio is a linear function of the total ozone, the slope and the intercept of these linear functions depend on the SZA. A linear relationship fit the data with a R^2 ranging between 0.87 and 0.99 for both sites. The distance between the lines increases with the increase of SZA. It can be noticed the ratio is about 2 for high sun and low column ozone while low ratios occur typically when the sun is low and total ozone is high in winter and erythemal UV is also low. Figures 4.35, 4.36 suggest that the ratio can be expressed ad a quadratic function of the solar zenith angle because of the dependence of the second order of UV irradiance by SZA (106). A polynomial of second degree relationship fit the data with with a R^2 ranging between 0.98 and 0.99 for both sites.

As expected by the previous analysis the ratio once again is about 2 for high sun and low column ozone, and it can be low when column ozone is large and the sun is low in the sky. In this case the distance between the lines is almost the same, revealing as SZA factor is more dominant compared to total ozone.

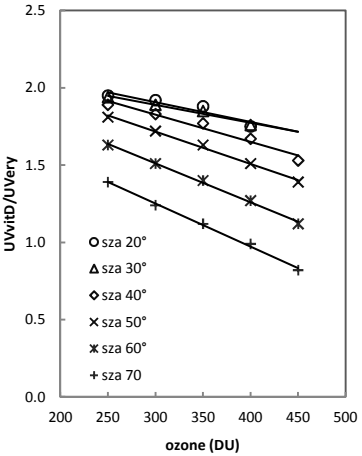

Figure 4.33 Mean ratio as a function of total ozone values for different SZAs at Rome. The solid lines indicate the linear fit.

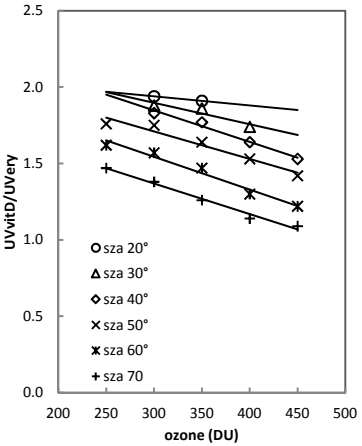

Figure 4.34 Mean ratio as a function of total ozone values for different SZAs at Aosta. The solid lines indicate the linear fit.

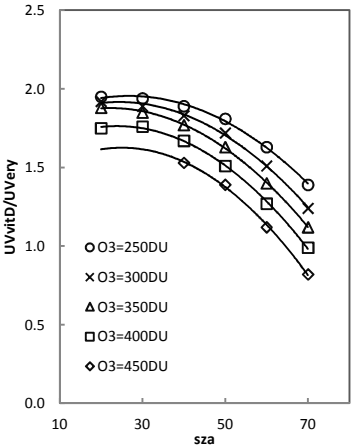

Figure 4.35 Mean ratio as a function of SZA for different total ozone amounts at Rome. The solid lines indicate the polynomial fit.

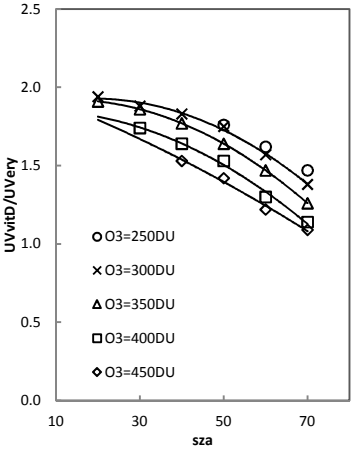

Figure 4.36 Mean ratio as a function of SZA for different total ozone amounts at Aosta. The solid lines indicate the polynomial fit.

4.8 Climatological Ratio as a function of SZA and Aerosol Index

The ratios (UV_{vitD}/UV_{ery}) were analyzed as a function of aerosol index fixing the total ozone amount, for different SZAs (20°÷70°) and are plotted in Figs 4.37, 4.38. Figures 4.39 and 4.40 show the ratios for different values of aerosol index. Data were binned with 0.5 increments for AI from -1 to 2.5 and with 10° increments for SZA from 20° to 70°.

The plots in fig 4.37 and 4.38 suggest that at each SZA the ratios do not show any changes related to AI variations

although the distance between the lines increase with the increase of SZA, revealing the dependence of the ratio by the SZA. The ratio is about 2 for high sun independently by AI values, it demonstrates that the SZA affect the ratios more than the AI.

Figures 4.39, 4.40 suggest that the ratio is a quadratic function of the solar zenith angle, due to the dependence of the second order of UV irradiance by SZA (106). A polynomial of second degree relationship fit the data with a R^2 ranging between 0.98 and 0.99 for both sites.

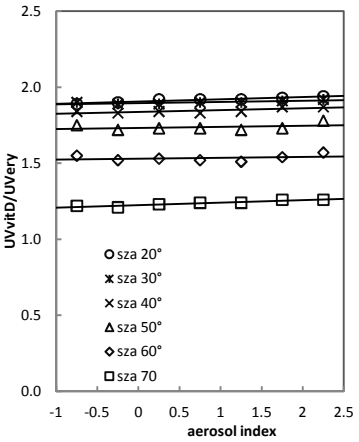

Figure 4.37 Mean ratio as a function of SZA and fixed value of aerosol index at Rome. The solid lines indicate the linear fit.

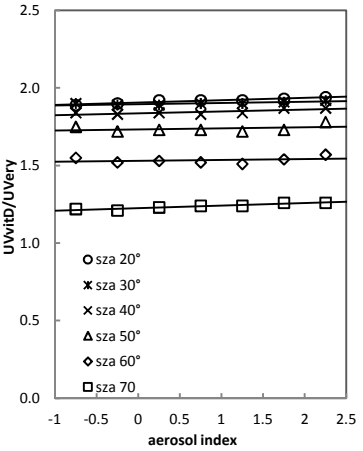

Figure 4.38 Mean ratio as a function of SZA and fixed value of aerosol index at Aosta. The solid lines indicate the linear fit.

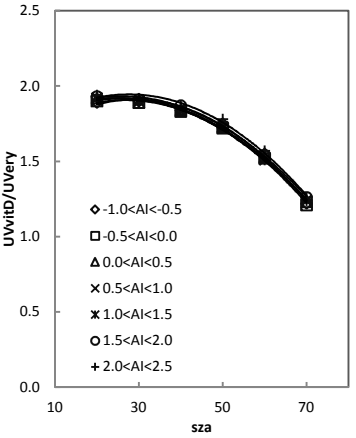

Figure 4.39 Mean ratio as a function of aerosol index and fixed SZA value of at Rome. The solid lines indicate the polynomial fit.

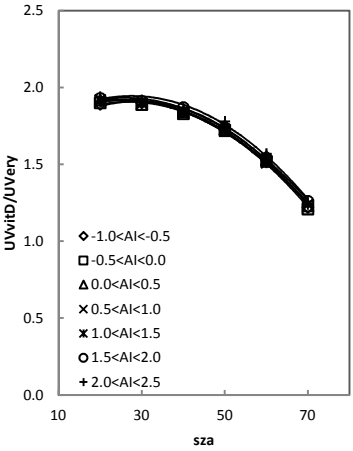

Figure 4.40 Mean ratio as a function of aerosol index and fixed SZA value of at Aosta. The solid lines indicate the polynomial fit.

4.9 Radiation Amplification Factor (RAF)

The sensitivity of erythemal and previtaminD_3 effective UV radiation to ozone change is investigated through the calculation of the Radiation Amplification Factor both for erythemal (RAF_{ery}) and vitamin D (RAF_{vitD}) as described in paragraph 3.5.

The strength of the relationship between modeled and biologically effective measured irradiances was investigated using Spearman's Rank correlation (R) for non-parametric

data. The range for a weak correlation was defined as zero to 0.29; a moderate correlation from 0.30 to 0.49 and a large correlation was defined as 0.50 or greater (113). Only RAF values with large correlation were considered.

The RAF values for total ozone in the range from 250 to 450 DU and erythemal UV irradiance are shown in Figures 4.41 and 4.42 at Rome and Aosta respectively.

The behavior of erythemal RAF with SZAs looks like slightly decreasing (within the uncertainty of the RAF_{ery}). The reason is that RAF behavior depends on the shape of the action spectrum. The erythemal action spectrum belongs to broadly – based action spectra group with exponentially decreases in the range 300-330 nm (114). At low SZAs, the most important erythemal contributing wavelengths are in the range of 300–330 nm where the ozone absorption is strong resulting in an enhanced sensitivity of erythemal effect to changes in atmospheric ozone.

At larger SZAs, the erythemal weights at longer wavelengths prevail and the UV_{ery} becomes less sensitive to ozone changes.

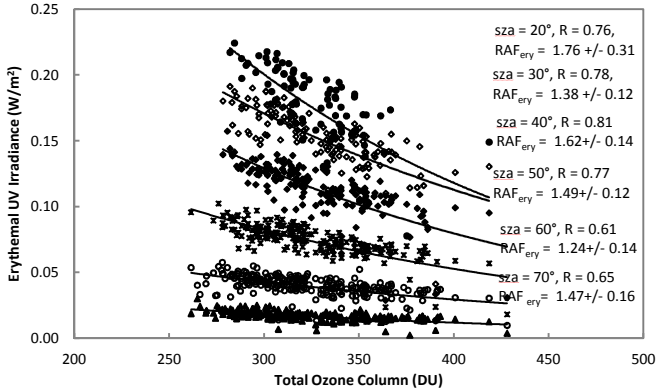

Figure 4.41 Determination of RAF for erythemal UV irradiance at SZA (20 ÷ 70)° and ozone value (250 ÷ 450 DU) at Rome. R is the Spearman coefficient.

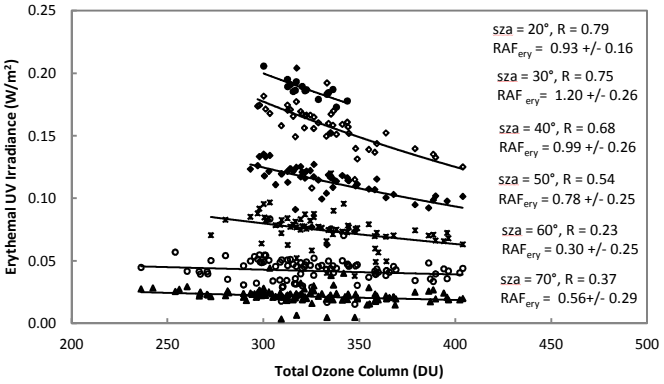

Figure 4.42 Determination of RAF for erythemal UV irradiance at SZA (20 ÷ 70)° and ozone value (250 ÷ 450) DU at Aosta. R is the Spearman coefficient.

The RAF_{ery} at Rome on the average are greater than at Aosta. At Rome 1% decrease in total column ozone would lead to 1.24-1.76 % increase in erythemal UV irradiance, with

maximum values reached at SZA = 20°. At Aosta 1% decrease in total column ozone would give 0.30-1.20 % increase in erythemal UV irradiance, with maximum values reached for SZA = 30° and minimum for SZA = 60°.

The values of RAF_{ery} at Rome are consistently higher than those found, using a transfer radiative model (93), at 30°N in Summer (small SZA and O_3 = 305 DU) of about 1.2 and of about 1.1 in Winter (large SZA and O_3 = 290 DU) and compared with those reported in the last Scientific Assessment of Ozone Depletion (2010) (58): for SZAs from 0° to 50° with typical mid-latitude ozone (300 DU) the RAF for erythemal effect ranges between 1.0-1.2, while for larger SZAs and larger ozone values the RAF decrease.

The higher RAF_{ery} values at the urban site of Rome are anyway consistent with those (RAF_{ery} = 0.4 ÷ 1.9) found at Seoul (37°N 126E°) (115). Moreover Herman et al. (2010) (116) reported RAF_{ery} at 40°N ranging between 0.8 ÷ 1.2 which are consistent with those found at Aosta.

Figures 4.43 and 4.44 show RAF_{vitD} at Rome and Aosta respectively. In contrast to erythema cases, RAF_{vitD} values increase with larger SZAs for both sites. It means that UV_{vitD} is more sensitive to ozone changes for large SZA. This behavior can again be understood from the shape of the action

spectrum which tends to zero for longer wavelengths and may be explained by the following considerations. The scattering due to the presence of aerosols, increases the length of the photon paths through the atmosphere. This effect is small when the scattered radiation is very small compared to the direct beam and stratospheric ozone changes are larger than those in troposphere. It might become significant for large solar zenith angles when a large fraction of the measured irradiance is due to diffuse radiation. However as pointed out by (114) is not clear if in the reality at large SZAs (i.e winter) a decrease of ozone produces (as determined by RAF_{vitD}) the actual biophysical processes or if it may be due to the lack of detection sensitivity in the experimental determinations of this spectrum

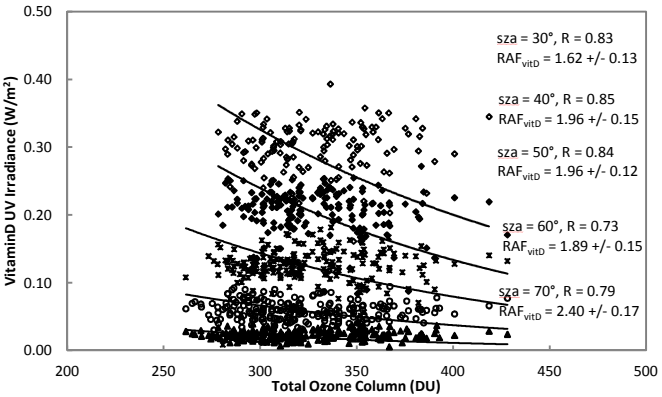

Figure 4.43 Determination of RAF_{vitD} for vitamin D UV irradiance at SZA (20 ÷ 70)° and ozone value (250 ÷ 450) DU at Rome. R is the Spearman coefficient.

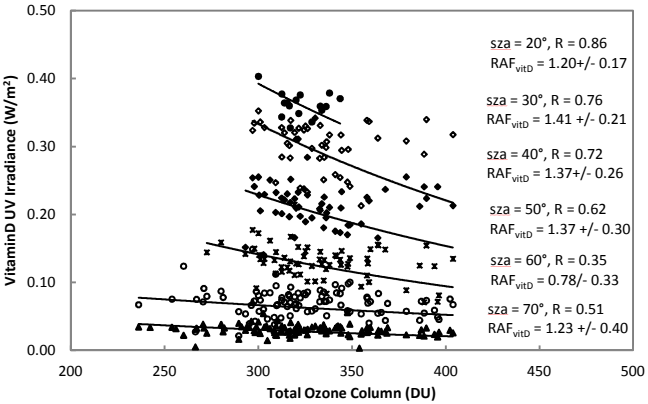

Figure 4.44 Determination of RAF_{vitD} for vitamin D UV irradiance at SZA (20 ÷ 70)° and ozone value (250 ÷ 450) DU at Aosta. R is the Spearman coefficient.

Also for vitamin D effects RAF_{vitD} values at Rome are greater than at Aosta, yielding that UV_{vitD} is less sensitive to ozone changes at the latter site. At Rome 1% decrease in total column ozone would give 1.62-2.40 % increase in pre-vitamin D_3 UV irradiance. At Aosta 1% decrease in total column ozone would give 0.78-1.41 % increase in pre-vitaminD_3 UV irradiance.

The RAF_{vitD} values at the Italian sites are consistent with those found at 40°N ranging between 1.4 ÷ 2.2 (116).

4.10 Exposure times for sufficient vitamin D versus erythema.

The climatological data of UV_{ery} and UV_{vitD} were used to calculate the optimum exposure times as function of UVI to get sufficient vitamin D without acquiring erythema.

4.10.1 Exposure time to induce erythema

Table A.1 in appendix A shows the time required to induce erythema as a function of UV index (UVI), for unprotected (SPF = 1) different skin types (II, III and IV) (see eq.3.12 in paragraph 3.6). It can be noticed that the times to get erythema are smaller for lighter skinned people. Melanin acts as a natural protective shield against the effects of UV radiation. People with dark skin have higher amounts of melanin and have greater natural protection from UV radiation. Blondes, redheads, and people with fair skins have less melanin and, therefore, burn more quickly.

For unprotected skin of type II, the times required to induce erythema around the maximum level of UVI (10 at Rome and 9 at Aosta) in summer, would be 19 min, while for unprotected skin of type IV, the time would be 33 min. In winter at local noon, when UVI is around 2-3, the time to induce erythema

for unprotected skin type II is about 1 hour and 20 minutes and for unprotected skin type IV is around 2 hours.

4.10.2 Calculation of exposure times for sufficient vitamin D

Tables A.2, A.3, A.4 and A.5 in appendix A show the exposure times to get sufficient vitamin D as function of UVI and areas of body exposed (see eq. 3.14 in paragraph 3.6). The Tables show as the time to get sufficient vitamin D increases for darker skinned people, because of the shield action that melanin performs against UV radiation.

For example we observe that for unprotected skin types II the time to get sufficient vitamin D for low UVI (2-3), which corresponds to noon on a mid-winter day at mid-latitudes when normally people expose only face and hands (A=0.1), is around 43 minutes. Under the same conditions for a skin types IV the required time is around 1 hour and 20 min. At noon on a summer day at mid-latitudes, which corresponds to a high UVI conditions, when normally people expose totally the body or the 63% of the total body, for unprotected skin types II and areas exposed between 1 and 0.63, the time to get sufficient vitamin D is around 1 min while for a skin types IV is around 2 min.

Moreover the time decreases with the increase of the body area exposed since the beneficial effects of UV radiation scale with the area of skin exposed (29).

At noon on a mid-winter day at mid-latitude, low UVI (between 2-3, and the ratio of UV_{VitD} /UV_{Ery} about 1.6), the time to achieve 1000 IU is about 1 h if only the hands and face (A=0.1) are exposed and about 6 min for full body exposure (A=1).In this season normally small areas of the body are exposed then the production of sufficient vitamin D in short time can be limited. At noon of a summer day , when UVI is typically about 8-10 (UVI "high") and the ratio is about 2, the time to produce a MED for skin type II is about 18 min, and the time to achieve 1000 IU is about 1 min for full body exposure (A = 1.0), and about 10 min if only the hands and face are exposed (A = 0.1).

Generally we can get sufficient vitamin D in less time than that required to induce erythema but we have to take in account that while normally in summer is always possible to get sufficient vitamin D by UV exposure at mid-latitudes, in winter, when only few areas of body are exposed, it is more difficult. Decreasing the exposed area the time to get sufficient vitamin D goes close to the time necessary to induce erythemal effect, hence the error associated to these

physiological relationship must be considered and then quantifying the optimal exposure time become more difficult.

Figure 4.45 depicts the calculated exposure times versus UV index at Rome. The area above the red line, indicating the eythema effect, provides times when erythema occurs on exposed skin for each UVI value. The area under the thick black lines, indicating the vitamin D effect for a full body exposure, gives the times when there is insufficient UV radiation to maintain optimal levels of vitamin D even for full body exposures. The other three curves give the approximate exposure times needed to maintain vitamin D for different areas of the body exposed. The picture shows that for full body exposures, there is a large difference between the time for sufficient UV and the time for too much UV. Decreasing the fraction of body exposed the difference between the time required to reach the optimum UV exposure and that to induce the erythema also decreases. If only hands and face are exposed, there is generally only a small gap between receiving insufficient UV for vitamin D production, and too much UV for skin damage (erythema). Similar pattern is experienced also for Aosta station.

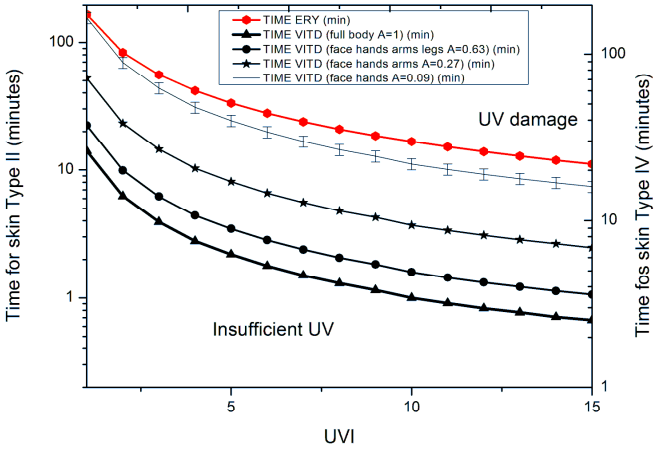

Figure 4.45 Range of the exposure times required for optimal UV plotted as a function of UVI.

4.11 Polysulphone Dosimetry Results

To investigate the use polysulphone dosimetry (PS) to retrieve vitamin D exposures, the climatogical ratios at Rome were used to determine first the coefficient c_{ery_mod} of the PS calibration curves then c_{vitD_mod} following the method described in chapter 3. The agreement between the retrieved c values were assessed with the comparison with those derived from calibration curves obtained from several field campaigns.

Tables 4.5, 4.6 report the values of the ratio (UV_{vitD}/UV_{ery}), and c_{ery_mod} and c_{vitD_mod} as a function of O_3 amounts (from 250 to 450 DU) and of SZA (from 20 to 70°). The ratio and theoretical coefficients are affected by an uncertainty equal to 10% due to uncertainty of spectral UV irradiance used in the calculation.

Ratio values higher than 1.90 are obtained for SZA ≤ 30° and O_3 ≤ 300 DU while values lower than 1.00 are obtained for SZA > 60° and O_3 ≥ 400 DU (Table 5.1). The results are in agreement with a similar study (106) based on a radiative transfer model.

RATIO	**SZA (°)**						
		20	**30**	**40**	**50**	**60**	**70**
O_3 (DU)	**450**			1.53	1.39	1.12	0.82
	400	1.75	1.76	1.67	1.51	1.27	0.99
	350	1.88	1.85	1.77	1.63	1.40	1.12
	300	1.92	1.89	1.83	1.72	1.51	1.24
	250	1.95	1.94	1.89	1.81	1.63	1.39

Table 4.5 The Ratios (UV_{vitD}/UV_{ery}) as a function of total O_3 and SZA at Rome site.

Tables 4.6 show that c_{vitD} is always higher than c_{ery} values because the pre-vitaminD_3 action spectrum is more sensitive to UVB region.

		C_{ery_mod} (kJm^{-2})						C_{vitD_mod} (kJm^{-2})					
		SZA (°)						SZA (°)					
		20	**30**	**40**	**50**	**60**	**70**	**20**	**30**	**40**	**50**	**60**	**70**
O_3 (DU)	**450**			0.86	0.82	0.77	0.75			1.32	1.14	0.86	0.62
	400	1	0.96	0.91	0.85	0.79	0.75	1.75	1.69	1.52	1.28	1.00	0.74
	350	1.06	1.02	0.96	0.90	0.82	0.77	1.99	1.89	1.70	1.47	1.15	0.86
	300	1.11	1.07	1.01	0.94	0.85	0.79	2.13	2.02	1.85	1.62	1.28	0.98
	250	1.19	1.15	1.08	0.99	0.89	0.82	2.32	2.23	2.04	1.79	1.45	1.14

Table 4.6 The c_{ery} and c_{vitD} coefficients as a function of total O_3 and SZA at Rome.

Table 4.7 reports the field campaigns listed in chronological order with sky conditions. The experimental c_{ery} and c_{vitD}. were obtained by the least squares regression method used for calibration curves. The c_{ery_mod} and c_{vitD_mod} values in Table 4.7 were determined as an average of the coefficients of Table 4.6 within the same range of SZA and ozone values experienced during each campaign.

Date	sky	c_{ery} (kJ m^{-2}) [R^2]	c_{ery_mod} (kJ m^{-2})	c_{vitD} (kJ m^{-2}) [R^2]	c_{vitD_mod} (kJ m^{-2})	SZA° (min-max)	O3 (DU)
24/05/04	scattered	1.04 ± 0.08 [0.83]	1.04 ± 0.10	2.35 ± 0.17 [0.83]	1.94 ± 0.19	21-34	368
22/07/04	clear	0.78 ± 0.03 [0.96]	1.09 ± 0.11	1.49 ± 0.06 [0.97]	2.07 ± 0.21	22-36	297
13/12/04	clear	0.93 ± 0.01 [0.98]	0.82 ± 0.08	0.93 ± 0.01 [1.00]	1.13 ± 0.11	65-70	298
04/02/05	clear	0.70 ± 0.02 [0.98]	0.82 ± 0.08	0.79 ± 0.03 [0.96]	1. 13 ± 0.11	58-70	312
20/07/05	clear	1.04 ±0.02 [0.98]	1.06 ± 0.11	1.96 ± 0.04 [0.98]	1.96 ± 0.11	21-57	265
28/07/05	scattered	1.05 ± 0.01 [0.98]	0.99 ± 0.10	1.78 ± 0.03 [0.99]	1.78 ± 0.18	23-58	300
08/06/06	scattered	0.80 ± 0.02 [0.98]	1.03 ± 0.10	0.85 ± 0.02 [0.96]	1.90 ± 0.20	19-51	283
26/05/2011	clear	1.17 ± 0.01 [0.996]	1.03 ± 0.10	2.23 ± 0.04 [0.99]	1.90 ± 0.20	21-53	323
27/05/2011	clear	1.15 ± 0.01 [0.996]	0.90 ± 0.10	1.98 ± 0.02 [0.996]	1.78 ± 0.18	22-66	318
12/07/2011	clear	0.62 ± 0.02 [0.97]	1.03 ± 0.10	1.16 ± 0.03 [0.98]	1.90 ± 0.20	20-51	290

Table 4.7 List of ten polysulphone field campaigns with the corresponding value of c coefficient (with the associated standard error) of calibration curve, fitted by a cubic polynomial function. R^2 is a measure of the goodness of the third degree polynomial fit.

The median and the interquartile range were used to describe the statistical distributions of the c values, which are not normally distributed. The median is a measure of the central tendency of a sample and the interquartile range is a measure of dispersion. Boxplots (figs. 4.46, 4.47) summarize the results

of the comparison between both c coefficients showing a reasonable agreement. The line inside every box depicts the median. The whiskers show minimum and maximum values within the data set that fall within an acceptable range. The top and bottom of the box mark the limits of ± 25% of the variable population.

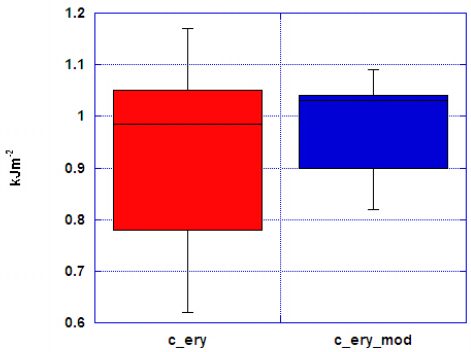

Figure 4.46 Comparison between theoretical and experimental values of c_{ery}.

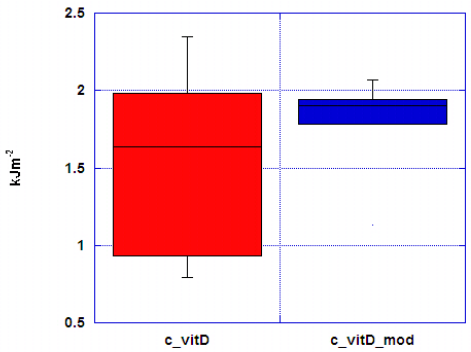

Figure 4.47 Comparison between theoretical and experimental values of c_{vitD}.

5 Discussion and conclusions

This study was stimulated by the somehow ambiguous role of solar ultraviolet (UV) radiation on human health, as well as by the lack of climatological UV characterization in Italy, in spite that in the last five years, 7000 deaths were attributed to solar UV exposure. The incidence of melanoma skin cancer between 1980 and 2000 increased by 4-8 percent per year. Non-melanoma skin cancers also increased during the last years (117).

Our main task was to provide information on the effects of the ambient UV radiation (i.e the incident biologically effective irradiance on a horizontal surface) as well as a reliable account of the risk/benefit balance of solar UV radiation. The results can be summarized under three items :

1. detailed analysis of experimental long term time series (climatology) of physical (ozone and aerosol index) parameters affecting the UV radiation at ground level in two distant sites in Italy (Rome and Aosta);
2. climatology based assessment of minimal/maximal values of physical parameters associated to risk/benefit thresholds for the two above mentioned sites;

3. validation of a polysulphone (PS) based dosimetric technique especially useful to quantify the biological effects of UV radiation in experimental field campaigns.

Notwithstanding the obvious interconnections, for the sake of clarity the three items will be separately considered in what follows.

5.1 Physical parameters affecting the UV radiation at ground level.

Table 5.1 reports the global information concerning the climatology of the physical variables of interest, namely total ozone and aerosol index (AI) in the absorbing ($AI_{abs}>0$) and non absorbing ($AI_{Nabs}<0$) modality (Cfr. Par. 4.1).

	ROME			AOSTA		
	Annual	**Maximal Values**	**Minimal Values**	**Annual**	**Maximal Values**	**Minimal Values**
Ozone (DU)	329.0 ± 8.0	351.5 ±15.4 (Spring)	304.7±8.1 (Fall)	329.8 ± 11.7	369.8±12.9 (Spring)	294.6 ± 7.7 (Fall)
AI_{abs}	0.69 ± 0.10	0.81 ± 0.07 (Winter)	0.50 ± 0.10 (Spring)	0.45 ± 0.09	0.50±0.22 (Spring)	0.34 ± 0.03 (Summer)
AI_{Nabs}	-0.36 ± 0.04	-0.41 ± 0.07 (Summer)	-0.33 ± 0.07 (Fall)	-0.43 ± 0.03	-0.52±0.04 (Summer)	- 0.30 ± 0.09 (Winter)

Table 5.1 Climatology of physical parameters influencing the ambient UV (i.e on horizontal surface) at two Italian sites. All values are given as means ± 1std .The ozone time-series of Rome and Aosta refer to the 1992- 2010 and 2007-2010 years, respectively (Cfr. Par. 4.1). The AI series cover the period 2004-2009 at Rome and 2007 -2010 at Aosta.

In the case of ozone, no significant difference has been observed between the two sites, which is not the case for both modalities of aerosol absorption. At the Rome site, in fact, it is noticeable that AI_{abs} and AI_{Nabs} values are higher and lower, respectively, as compared to the Aosta Site. The former point is easily accounted for by the higher urban pollution (Rome); the latter point, actually limited to maximal values, is most probably due to the higher frequency of cloudy days registered at Aosta. Among the three physical parameters listed in Table 5.1, the total ozone showed larger biological effects (Cfr. Par. 4.6, 4.8). However, the lack of difference between the two sites is in agreement with the similar estimate of exposure-time thresholds for biological effects at the two sites (Cfr.Par. 4.10 and the Appendix A).

The peculiar seasonal variability of three parameters, taken together with the multi-year series of high quality spectral UV measurements at Rome (1996-2009) and Aosta (2007-2010), is an important clue to rationalize the seasonal variability of two biologically effective quantities, namely Vitamin D dose rate (UV_{vitD}) and erythemal dose rate (UV_{ery}) at three day times: 11 UTC (local noon), 8 UTC and 15 UTC (beginning and end of the working time windows for the majority of the population). As a matter of fact, taking into account all sky

conditions, UV_{ery} and UV_{vitD} climatologies show typical seasonal behaviour with peak values in Summer around local noon, due to the combined effect of lower total ozone and solar zenith angle (Table 5.2).

	ROME			AOSTA		
	Peak values	Mean values (Winter)	Mean values (Summer)	Peak values	Mean values (Winter)	Mean values (Summer)
UV_{ery} (mW/m^2)	251.2 (11UTC)	37.7±23.0 (15UTC)	95.8±64.7 (11UTC)	232.5 (11 UTC)	28.5±26.2 (15UTC)	87.5±62.3 (11UTC)
UV_{vitD} (mW/m^2)	480.4 (11UTC)	57.1±39.5 (15UTC)	173.9±127.8 (11UTC)	453.1 (11UTC)	43.6±45.9 (15UTC)	157.8±124.1 (11UTC)
UV_{vitD}/UV_{ery}	1.9	1.5	1.8	1.9	1.5	1.8

Table 5.2 Biological effective quantities affected by the UV radiation at two Italian sites. For both sites the peak values refer to data collected in Summer at the indicated day time (UTC), and the mean values (± std) refer to data collected under all sky conditions.

At both sites UV_{vitD} is higher than UV_{ery} of about a factor 2 in peak values and throughout Summer (around noon), while in Winter the UV_{vitD}/UV_{ery} drops to 1.5. In Winter, in fact, the increased optical path of solar irradiance through the atmosphere (i.e higher solar zenith angles) and the enhanced scattering lead to a much stronger reduction of UV_{vitD} as compared to UV_{ery}, due to the larger sensitivity of the pre-vitamin D_3 action spectrum to the UVB region. As a consequence, it is not unusual at low Winter SZAs (see Table 4.4 and Figures 4.27 e 4.28) that the erythemal effect prevails and may somehow inhibit the production of vitamin D. Thus, the large seasonal variability in UV radiation, taken together

with the season-dependent changes in the personal exposure to UV radiation of many people, for working or leisure activities, may have important implications for human health.

5.2 Risk/benefit thresholds for human health.

Based on the UV_{ery} series, the climatology of the UV Index (an indicator of damaging UV levels calculated dividing UV_{ery} by 25 mW/m^2) at local noon at both sites is provided in the Results (Cfr. Par. 4.4). The occurrences of high UV Indexes is in Summer while low values are in Winter. It is noticeable that the fraction of events above the risk threshold level is higher in Aosta than in Rome (Table 5.3).

	Very high 10<UVI<8	**High 6<UVI<7**	**Low 0<UVI<2**
ROMA	3.4	33.0	36.0
AOSTA	4.1	33.8	31.6

Table 5.3 Percent of daily maximal values of UV index. Notice that the risk threshold level is 3 and the three reported classes are related to the level 0-2 (low), 6-7 (high), >8 (very high). (85).

In any case, UV exposure protection measures should be strongly recommended at both sites in Summer.

Looking at the beneficial UV effect it was found that at the two Italian sites Vitamin D photo-production can be sustained

at local noon during the whole year, except for overcast sky conditions when the attenuation is very strong (see Tab. 5.4).

	UV_{vitD} > 3.46 mW/m^2 (%)			UV_{vitD} < 3.46 mW/m^2 (%)		
	08 UTC	**11 UTC**	**15 UTC**	**8 UTC**	**11 UTC**	**15 UTC**
Rome	94.2	99.6	95.3	5.8	0.4	4.7
Aosta	79.3	99.5	77.6	20.7	0.5	22.4

Table 5.4 Day time dependence of events above and below the threshold for cutaneous production of vit D. The threshold value of 3.46 mW/m^2 (50) is reached at both sites throughout the year at noon (see Par. 4.4).

Our analysis of climatologies demonstrated that at each SZA the UV_{vitD}/UV_{ery} ratios show no significant change related to aerosol index (AI), revealing that the SZA is more critical also when compared to AI. More precisely, high ratios tend to occur for smaller SZA when the atmospheric attenuation is strongly reduced, and at fixed SZA the climatologies of ratio are mainly affected by the total ozone column. The maximal ratio values, for a fixed SZA value, are in fact observed in Fall (when ozone is low), while the minimum is experienced in Spring (when the ozone amounts are large). Further analysis demonstrated that the UV_{vitD}/UV_{ery} ratio is a linear decreasing function of the total ozone for fixed SZA, while it is a quadratic function of the SZA for fixed values of ozone (paragraph 4.7), confirming that SZA is a dominant factor compared to ozone (12).

The climatologies also allowed to estimate recommended UV exposure times (cloudless sky) to produce an optimal vitamin D level (t_{vitD}), without inducing the erythemal effect ($t_{vitD} < t_{ery}$) as a function of UV index (UVI) around local noon and for different areas of the body exposed (A).

Table 5.5 summarizes the exposure time calculated for low and high UV indexes as previously described (paragraph 4.4 and 4.10) and reported in the Appendix A.

	ROME				AOSTA			
	UVI=9		UVI=1		UVI=10		UVI=1	
	Phototype II	Phototype IV	Phototype II	Phototype IV	Phototype II	Phototype IV	Phototype II	Phototype IV
t_{ery}	19	33	167	300	17	30	167	300
t_{vitD} (A=1.0)	1	2	14	25	1	2	15	27
t_{vitD} (A=0.63)	2	3	22	40	2	3	24	43
t_{vitD} (A=0.27)	4	8	52	94	4	7	56	100
t_{vitD} (A=0.10)	13	23	156	282	11	20	167	301

Table 5.5 Exposure times for erythema and optimal vitamin D production for different skin types. The times (in minutes) are reported for maximal and minimum UV indices at both sites. Different fractions of the exposed body areas were taken into account: A= 1 (full body); A= 0.63 (only face, hands, arms and legs); A=0.27 (face, hands and arms); A=0.10 (hands and face).

The time differences for photosynthesizing optimal vitamin D for low UVI between the two sites is due to the different ratio (UV_{vitD}/UV_{ery}) at the two sites (see paragraphs 4.7) while those for high UVI depend on the different peak values experienced at the two sites.

It ought to be noticed that besides environmental factors like air pollution, surface albedo, altitude, also the skin orientation relative to the Sun and the geometry of the human body, could strongly modify the results confined to UV irradiance measurements on horizontal surface.

The reported optimal exposure times are only approximate: the estimate, in fact, is based on the radiation on a horizontal surface, with no consideration of all the inclined body surfaces. This is irrelevant however, in the estimate of the relative differences among different phototypes, due to the shield action of melanin against UV radiation. Thus, Blondes, redheads, and people with fair skins (lower phototypes) have less melanin and, therefore, burn more quickly and need longer times to get sufficient Vitamin D (Figs. 4.45). Needless to say, since the beneficial effects of UV radiation scale with the area of the exposed skin, the time to get sufficient vitamin D decreases with the increase of the exposed body area for all phototypes.

However, when a small fractional area of the body is exposed, there is a small difference between the time to induce the erythemal effect and the time to get sufficient vitamin D. In this cases to quantify the optimal exposure time become more difficult and the error associated to these physiological

relationship must be considered. Although a direct comparison between the Italian exposure times for sufficient vitamin D and those obtained by McKenzie et al. (29) at Lauder in New Zealand, is difficult due to the specific characteristics (ozone, surface albedo, aerosol contents) of the two sites, it can be noticed an amazing consistency in the case of skin type II and under high UVI conditions: at a full-body exposure, around 15 minutes at the Italian sites against 20 minutes at Lauder; at 10% of body exposure, 160 min at Italian sites and 200 minutes at Lauder.

As a conclusion, our results suggest a large body area exposure for short times at low values of UVI (e.g., in summer, when the sun is low) as optimal conditions of UV exposure. It should be noticed that at middle latitudes it is always possible in summer to get sufficient vitamin D by UV exposure; in winter, however, due the low temperature and the small exposed body-areas, it is more difficult to get sufficient vitamin D production at no erythemal risk.

The sensitivity of erythemal and previtaminD_3 effective UV radiation to ozone change was investigated also through the calculation of the Radiation Amplication Factor both for erythema (RAF_{ery}) and vitamin D (RAF_{vitD}).

	Rome	Aosta
RAF_{ery}	1.76 (20°) ; 1.24 (60°) ;	1.20 (30°)* ; 0.78 (50°)
RAF_{vitD}	1.62 (30°) ; 2.40 (70°) ;	*1.20 (20°) ; 1.37 (50°)*

Table 5.6 RAFs for the two sites under study. The reported values refer to minimum and maximum RAF values at high and low SZA (in parenthesis) with R correlation > 0.50 .

Given the recent discussions on the reduction of stratospheric ozone and the ensuing increase in ultraviolet radiation reaching the biosphere, the RAF parameter (to be interpreted as the percentage increase in biologically active irradiance resulting from 1% decrease in the ozone column), is worth of specific interest. Table 5.6 summarizes the RAF estimates with correlation coefficients > 0.5 between experimental and model data, reported in Par. 4.9 from climatology data. Due to its definition ($RAF= - d\ lnI_{bio}/d\ lnO_3$, where I_{bio} is the biologically active irradiance), the amplification factor of biological effects of UV radiation should decrease with increasing of the (shielding) O_3 column length in the stratosphere, and hence with increasing SZA: this is what actually occurs for erythemal effects (RAF_{ery}) at both sites. A possible explanation of the opposite trend observed for RAF_{vitD}, is the steeper dependence of the vitamin D action spectrum (as compared to the erythemal one) for the wavelength range (310 – 330 nm) where the O_3 shielding effect is substantial. Moreover, it is difficult to estimate in this context the possible role of specific and largely unknown

photochemical mechanisms finely tuned – and hence highly sensitive – to any irradiance change at specific wavelengths.

As for the consistently higher RAF values at the urban site of Rome as compared to Aosta under all conditions, it appears linked to the bulk of diffusion and scattering phenomena caused by tropospheric aerosol and pollutants and still neglected in any available models of RAF calculations from experimental data.

5.3 A polysulphone-based dosimetric technique of general use.

The outcomes of the climatological analysis allowed to check the applicability of a new method to derive vitamin D dose based on polysulphone dosimetry, normally used to measure erythemal effects only, and hence to extend the potentiality of the PS dosimetric technique.

Based on the high-quality UV irradiances measured by Brewer, the calibration curves coefficients c_{ery_mod} and c_{vitD_mod} were retrieved as a function of O_3 amounts (from 250 to 450 DU) and SZA (from 20 to 70°) (see par 4.11). Once again, c_{vitD_mod} is higher than c_{ery_mod} since the pre-vitaminD_3 action spectrum is more sensitive to the UVB region. Such values

were found in good agreement with the c_{vitD} and c_{ery} coefficients retrieved (by a least squares regression) from calibration curves obtained during ten experimental campaigns in the field (see the Box-plots in Par 4.11) and summarized in Table 5.7.

	c_{ery_mod} (kJm^{-2})	c_{ery} (kJm^{-2})	c_{vitD_mod} (kJm^{-2})	c_{vitD} (kJm^{-2})
Median	1.03	0.99	1.90	1.64
Min, Max	0.82, 1.09	0.62, 1.17	1.00, 2.07	0.79, 2.35

Table 5.7 Median, minimum and maximum of experimental c_{ery} and c_{vitD} coefficients obtained during 10 dosimetric field campaigns as compared to theoretical c_{vitD_mod} and c_{ery_mod} coefficients.

These results are of relevant practical importance in so far as they make it possible:

- to derive pre-vitaminD_3 doses from erythemal doses obtained in past dosimetric field campaigns;
- to retrieve pre-vitaminD_3 dose rates from broad-band UV radiometers, which only provide erythemal dose rates;
- to extend polysulphone dosimetry for synchronous estimates of erythemal and pre-vitaminD_3 doses received by people exposed to solar UV radiation. Such an approach would minimize the personal discomfort, due to the small weight of PSA dosimeters, and considerably improve the experimental accuracy, due to the easy application of dosimeters to any anatomical site.

Appendix A - Time exposure to induce erythema and for sufficient vitamin D

Time for erythema (min)			
UVI	**Skin Type II**	**Skin Type III**	**Skin Type IV**
1	167	233	300
2	83	117	150
3	56	78	100
4	42	58	75
5	33.	47	60
6	28	39	50
7	24	33	43
8	21	29	38
9	19	26	33
10	17	23	30

Table A.1 Range of UVI and corresponding exposure times for erythema for different skin types.

			Time for 1000 IU VitD (min) (full body A=1.0)					
	Ratio (UV_{VitD}/UV_{Ery})		Skin Type II		Skin Type III		Skin Type IV	
UVI	**Rome**	**Aosta**	**Rome**	**Aosta**	**Rome**	**Aosta**	**Rome**	**Aosta**
1	1.42	1.33	14	15	20	21	25	27
2	1.60	1.60	6	6.	9	9	11	11
3	1.70	1.67	4	4	6	6	7	7
4	1.80	1.79	3	3	4	4	5	5
5	1.83	1.82	2	2	3	3	4	4
6	1.87	1.90	2	2	3	3	3	3
7	1.90	1.93	2	2	2	2	3	3
8	1.93	1.93	1	1	2	2	2	2
9	1.93	1.93	1	1	2	2	2	2
10	2.00	2.00	1	1	1	1	2	2

Table A.2 Range of UVI and corresponding exposure times for photosynthesizing optimal vitamin D for different skin types for a full body exposure at Rome and Aosta.

			Time for 1000 IU VitD (min) (face hands arms legs A=0.63)					
	Ratio (UV_{VitD}/UV_{Ery})		Skin Type II		Skin Type III		Skin Type IV	
UVI	**Rome**	**Aosta**	**Rome**	**Aosta**	**Rome**	**Aosta**	**Rome**	**Aosta**
1	1.42	1.33	22	24	31	33	40	43
2	1.60	1.60	10	10	14	14	18	18
3	1.70	1.67	6	6	9	9	11	11
4	1.80	1.79	4	4	6	6	8	8
5	1.83	1.82	4	4	5	5	6	6
6	1.87	1.90	3	3	4	4	5	5
7	1.90	1.93	2	2	3	3	4	4
8	1.93	1.93	2	2	3	3	4	4
9	1.93	1.93	2	2	3	3	3	3
10	2.00	2.00	2	2	2	2	3	3

Table A.3 Range of UVI and corresponding exposure times for photosynthesizing optimal vitamin D for different skin types for exposing face, hands, arms and legs at Rome and Aosta.

			Time for 1000 IU VitD (min) (face hands arms A=0.27)					
	Ratio (UV_{VitD}/UV_{Ery})		Skin Type II		Skin Type III		Skin Type IV	
UVI	**Rome**	**Aosta**	**Rome**	**Aosta**	**Rome**	**Aosta**	**Rome**	**Aosta**
1	1.42	1.33	52	56	73	78	94	100
2	1.60	1.60	23	23	32	32	42	42
3	1.70	1.67	15	15	20	21	26	27
4	1.80	1.79	10	10	14	15	19	19
5	1.83	1.82	8	8	11	11	15	15
6	1.87	1.90	7	7	9	9	12	12
7	1.90	1.93	6	6	80	8	10	10
8	1.93	1.93	5	5	7	7	9	9
9	1.93	1.93	4	4	6	6	8	8
10	2.00	2.00	4	4	5	5	7	7

Table A.4 Range of UVI and corresponding exposure times for photosynthesizing optimal vitamin D for different skin types for exposing face, hands and arms at Rome and Aosta.

			Time for 1000 IU VitD (min) (face hands A=0.10)					
	Ratio (UV_{VitD}/UV_{Ery})		Skin Type II		Skin Type III		Skin Type IV	
UVI	**Rome**	**Aosta**	**Rome**	**Aosta**	**Rome**	**Aosta**	**Rome**	**Aosta**
1	1.42	1.33	156	167	219	234	282	301
2	1.60	1.60	69	69	97	97	125	125
3	1.70	1.67	44	44	61	62	78	80
4	1.80	1.79	31	31	43	43	56	56
5	1.83	1.82	24	24	34	34	44	44
6	1.87	1.90	20	19	28	27	36	35
7	1.90	1.93	17	16	23	23	30	30
8	1.93	1.93	14	14	20	20	26	26
9	1.93	1.93	13	13	18	18	23	23
10	2.00	2.00	11	11	16	16	20	20

Table A.5 Range of UVI and corresponding exposure times for photosynthesizing optimal vitamin D for different skin types for exposing face and hands at Rome and Aosta.

Acronyms

A	Percentage of total body area exposed
AI	Aerosol Index
AI_{abs}	Absorbing Aerosol Index (> 0)
AI_{Nabs}	Non-Absorbing Aerosol Index (< 0)
ARPA VDA	Environmental Agency of Aosta Valley
AS	All Sky conditions
BCC	Basal Cell Carcinoma
BPS	Brewer Processing Software
CIE	Commission Internationale de l'Eclairage
CMM	Cutaneous Malignant Melanoma
CS	Clear Sky conditions
7-DHC	7-Dehydrocholesterol
$(1,25(OH)_2D)$	1,25-Dihydroxyvitamin D
DU	Dobson Unit
EQT	Equation of Time
ETC	Ozone Extra-Terrestrial Constant
FWHM	Full Bandwidth at Half Maximum
25(OH)D	25-hydroxyvitamin D
IARC	International Agency for Research on Cancer
IU	International Unit
MED	Minimal Erythemal Dose
NMSC	Non Melanoma Skin Cancer
O_{3norm}	Climatological Daily Total Ozone Amounts
OMI	Ozone Monitoring Instrument

PS	Polysulphone
PTH	Parathyroid Hormone
RAF	Radiation Amplification Factor
R_n	Earth-Sun Distance
SCC	Squamous Cell Carcinoma
SDD	Standard Vitamin D Dose
SED	Standard Erythemal Dose
SPF	Sun Protection Factor
SZA	Solar Zenith Angle
TOMS	Total Ozone Monitoring Spectrophotometer
UCEA	Central Office Agrarian Ecology
UTC	Universal Time Clock
UV	Ultraviolet
UVA	Ultraviolet Radiation A (400-320 nm)
UVB	Ultraviolet Radiation A (320-290 nm)
UVC	Ultraviolet Radiation A (290-200 nm)
UVI	Ultraviolet Index
UVR	Ultraviolet Radiation (200-400 nm)
UV_{bio}	Biologically Effective Radiation
UV_{ery}	Erythemal Dose Rate
UV_{vitD}	Vitamin D Dose Rate
WOUDC	World Ozone and Ultraviolet Data Center

Scientific Publications

- Siani A.M., Modesti S., Casale G.R., Diemoz H., Colosimo A., *"Biologically effective surface UV climatology at Rome and Aosta, Italy"* to be submitted to Photochem. and Photob., **2012**.
- Siani A.M., Casale G.R., Modesti S., Colosimo A., "*Solar UV Radiation as a Double Face Environmental Pollutant."* In: Urban Pollution: Physical and Chemical Agents. Rome, Italy, March 25, **2010**, vol. 3(1), p. 13-20, ISBN/ISSN: 2037-0199.

Proceedings

- Siani A.M., Modesti S., Casale G.R., Diemoz H., Colosimo A., *"Biologically effective surface UV climatology at Rome and Aosta, Italy"* submitted to IRS2012- International Radiation Symposium 2012, Berlin, Germany, 06 – 10 August **2012**.
- Modesti S., Casale G.R., Siani A.M., Colosimo A., *"Studio della radiazione ultravioletta biologicamente efficace (produzione vitamina D ed eritema) in funzione dei parametri atmosferici"*, XCVII Congresso Nazionale SIF (Società Italiana di Fisica), L'Aquila, 26-30 September **2011**.
- Siani A.M., Casale G.R., Modesti S.: *"U-Rome Ozone Series Reprocessing"*, 13th Biennal WMO-GAW Brewer Users Group Workshop, Chinese Academy of Meteorological Science (CAMS) and the Chinese

Meteorological Administration (CMA), Bejing, China, 12-16 September **2011**.

- Modesti S., Siani A.M., Casale G.R., *"A characterization of human erythemal and Vitamin D exposure from UV radiation measurements at Rome station"*, XIX Congress of the Carpathian Balkan Geological Association, CBGA 2010, (Thessaloniki, GR) 23-26 September **2010**.
- Siani A.M., Casale G.R., Modesti S., Colosimo A., *"Studio della radiazione UV: il punto di vista del fisico"*, 7° Edizione Convegno Nazionale SANIT Forum Internazionale della Salute, 22-25 June **2010**.
- Siani A.M., Casale G.R., Modesti S., *"Sole ed Ambiente"*, 6° Edizione Convegno Nazionale SANIT Forum Internazionale della Salute, 23-26 June **2009**.

Experimental Field Campaigns

- Marine Site Field Campaign (Orbetello (GR)) on the quantification of the personal UV dose and colorimetric skin measurements. June **2011**
- ARPA VDA Field Campaign on the UVR characterization at high altitude and glacial site (Plateau Rosa (AO), 3500 m s.l.m.) as a function of the environmental and atmospheric factors and on the personal exposure in extreme UVR ambient. July **2010**.

Bibliography

1. www.radiazioneuv.org. [Online]

2. www.rebootyourbody21.com. [Online]

3. Influence of season and latitude on the cutaneous synthesis of vitamin D3: exposure to winter sunlight in Boston and Edmont will not promote vitamin D3 synthesis in human skin. ***Webb A. R., L. Kline and M. F. Holick.*** *1988, J. Clin. Endocrinol. Metab., Vol. 67, pp. 373-378.*

4. Sunlight regulates the cutaneous production of vitamin D3 by causing its photodegradation. ***Webb A.R., B.R. DeCosta and M.F. Holick.*** *1989, J. Clin. Endocrinol. Metab. , Vol. 68, pp. 882–887.*

5. Vitamin D deficiency. ***Holick M.F.,.*** *2007, N. Engl. J. Med., Vol. 357, pp. 266-281.*

6. Benefits and requirements of vitamin D for optimal health: a review. ***Holick M.F., Grant W.B. and.*** *2, s.l. : Sunlight Nutrition and Health Research Center (SUNARC), wgrant@sunarc.org., 2005, Altern Med Rev., Vol. 10, pp. 94-111.*

7. Photoprotection and vitamin D status. ***Springbett P., S. Buglass and A.R. Young.*** *2, s.l. : Elsevier B.V., Photochem. and Photobiol., Vol. 101, pp. 160-168. http://www.ncbi.nlm.nih.gov/pubmed/20444619.*

8. Ultraviolet Radiation. ***WHO,*** *World Health Organization. Geneve, Switerzland : s.n., 1994. Techn. Rep.*

9. What is light? ***Diffey B.L,.*** *2, 2002, Photoderm., Photoimm. & Photomed., Vol. 18, pp. 68-74. DOI: 10.1034/j.1600-0781.2002.180203.x.*

10. Uncertainties in modeled UV-irradiances due to limited accuracy and availability of input data. ***Schwander H., P. Koepke and A. Ruggaber.*** *D8, 1997, J. Geophys. Res., Vol. 102, pp. 9419 – 9429.*

11. Large losses of total ozone in Antarctica reveal seasonal CLOx/NOx interaction. ***Farman J.C., B.G. Gardiner and Shanklin.*** *1985, Nature, Vol. 315, pp. 207-10.*

12. Variability of UV Irradiance in Europe. ***Seckmeyer G., D.Pissulla, M.Glandorf, D.Henriques, B.Johnsen, A.Webb, A.M.Siani, A.Bais, B.Kjeldstad, C.Brogniez, J.Lenoble, B.Gardiner, P.Kirsch, T.Koskela, J.Kaurola, B.Uhlmann, H.Slaper, P.den Outer, M.Janouch, P.Werle, A.de la Casiniere and S.Simic.*** *2008 : s.n., Photochem. and Photob., Vol. 84, pp. 172–179.*

13. Modification of Global Erythemally Effective Irradiance by Clouds. ***Thiel S., K. Steiner and H. K. Seidlitz.*** *6, 1997, Photochem and Photobiol, Vol. 65, pp. 969-973. DOI: 10.1111/j.1751-1097.1997.tb07956.x.*

14. The impact of biogenic carbon sources on aerosol absorption in. ***Marley N.A., JA. Marley, J.S. Gaffney, M. Tackett, N.C. Sturchio, L. Heraty, N. Martinez, K. D. Hardy, A. Marchany-Rivera, T. Guilderson, A. MacMillan, and K. Steelman.*** *2009, Atmos. Chem. Phys, Vol. 9, pp. 1537–1549.*

15. Black carbon or brown carbon? The nature of light-absorbing. ***Andreae M.O. and A. Gelencsér.*** *2006, Atmos. Chem. Phys., Vol. 6, pp. 3131–3148.*

16. Spectral absorption properties of atmospheric aerosols. ***Bergstrom R.W., P. Pilewskie, P.B. Russell, J. Redemann, T.C. Bond, P.K. Quinn and B. Sierau.*** *23, 2007, Atmos. Chem. Phys., Vol. 7, pp. 5937-5943.*

17. Transmittance of a cloud is wavelenght-dependent in the UV-range. ***Seckmeyer G., R. Erb and A. Albold.*** *1996, Geophys. Res. Lett., Vol. 23, pp. 2753-2755.*

18. Scientific Assesment of Ozone Depletion: 2006. ***WMO,*** *World Meteorological Organization. Geneva, Switzerland. : s.n., 2007. Global Ozone Research and Monitoring Project– Report No. 50.*

19. Reflected solar radiation from horizontal, vertical and inclined surfaces: Ultraviolet and visible. ***Turner J., A.V. Parisi and D.J. Turnbull.*** *1, 2008, Photochem. and Photob., Vol. 92 , pp. 29-37. doi: 10.1016/j.jphotobiol.2008.03.006.*

20. Measurements of spectral snow albedo at Neumayer, Antartica. ***Wuttke S., G. Seckmeyer, and G. König-Langlo.*** *2006, Ann. Geophys. , Vol. 24, pp. 7-21.*

21. Diurnal variations in the UV albedo of arctic snow. ***Meinander O., A. Kontu, K. Lakkala, A. Heikkilä, L. Ylianttila, and M. Toikka.*** *21, 2008, Atmos. Chem. Phys., Vol. 8, pp. 6551-6563. doi: 10.5194/acp-8-6551-2008.*

22. First national intercomparison of solar ultraviolet radiometers in Italy. ***Diemoz H., A. M. Siani, G. R. Casale, A. di Sarra, B. Serpillo, B. Petkov, S. Scaglione, A. Bonino, S. Facta, F. Fedele, D. Grifoni, L. Verdi, and G. Zipoli.*** *2011, Atmos. Meas. Tech., Vol. 4, pp. 1689–1703.*

23. Measurements of spectral solar UV irradiance in tropical Australia. ***Seckmeyer G., Bernhard G. and.*** *D7, 2007, J. Geoph. Res. , Vol. 102, p. 1997.*

24. "The wavelengths in sunlight effective in producing skin cancer: a theoretical analysis". ***Setlow R.B.,*** *9, 1974, Proc. Nat. Acad. Sci., USA,, Vol. 71, pp. 3363-3366.*

25. Joint ISO / CIE Standard: Erythema Reference Action Spectrum and Standard Erythema Dose. ***CIE.*** *1999, ISO 17166/CIE S007/E-1999.*

26. A reference spectrum for ultraviolet induced erythemal in human skin. ***Diffey A.F., and B.L. McKinlay.*** *1987, CIE J., Vol. 6, pp. 17-22.*

27. Wavelengths effective in induction of malignant melanoma. ***Setlow R.B., E. Grist, K. Thompson and A.D. Woodhead.*** *1993, Proc. Natl. Acad.USA, Vol. 90, pp. 6666–6670.*

28. Changes in biologically active ultraviolet radiation reaching the Earth's surface. ***Madronich S., R.L. McKenzie, L.O. Bjorn, M.M. Caldwell.*** *1998, Photochem and Photob, Vol. 46, pp. 5–19.*

29. UV Radiation: Balancing Risks and Benefits. ***McKenzie R.L., J. B. Liley and L. O. Bjorn.*** *2008, Photochem. Photobiol., Vol. 85, pp. 88–98. DOI: 10.1111/j.1751-1097.2008.00400.x.*

30. The validity and practicality of Sun-reactive skin types I through VI. ***Fitzpatrick T. B,.*** *1998, Arch. Dermatol., Vol. 124, pp. 869–871.*

31. Personal UV exposure in high albedo alpine sites. ***Siani A.M., G. R. Casale, H. Diémoz, G. Agnesod, M.G. Kimlin, C.A. Lang, and A. Colosimo.*** *2008, Atmos. Chem. Phys., Vol. 8, pp. 3749–3760.*

32. Polysulphone dosimetry: a tool for a personal exposure studies. ***Casale G.R, A.M. Siani and A. Colosimo.*** *1, 2009, Biophys. & Bioeng. Letters , Vol. 2.*

33. Photoaging of the skin. ***Ichihashi M., H. Ando, M. Yoshida, Y. Niki and M. Matsui.*** *6, 2009, Anti-aging Medicine, Vol. 6, pp. 46-59.*

34. Photoaging. Manifestations, prevention, and treatment. ***Kligman L.H,.*** *3, 1986, Dermatol Clin, Vol. 4, pp. 517-28.*

35. The role of near infrared radiation in photoaging of the skin. ***Schroeder P., J. Haendeler and J. Krutmann.*** *7, 2008, Experimental gerontology, Vol. 43, pp. 629–632.*

36. Solar Ultraviolet Radiation: Global burden of disease from solar ultraviolet radiation. ***WHO.*** *World Health Organization, Public Health and the Environment. Geneva, switzerland : Prüss-Üstün A., H. Zeeb, C. Mathers, M. Repacholi, 2006.*

37. ***ICNIRP, International Commission on Non-Ionizing Radiation Protection.*** Protecting Workers from Ultraviolet Radiation. *2007. pp. 25-27.*

38. An epidemiological perspective of ultraviolet exposure--public health concerns. ***Lucas R.M.,*** *4, 2011, Eye Contact Lens, Vol. 37, pp. 168-75.*

39. Estimating the global disease burden due to ultraviolet radiation exposure. ***Lucas R.M., A.J. McAnthony, B.K. Armstrong and W.T.Smith.*** *3, 2008, Int. J. Epidemiol. , Vol. 37, pp. 654-667. doi: 10.1093/ije/dyn017.*

40. The effects of ultraviolet radiation on the human immune system. ***Duthie, Kimber and Norval.*** *6, 1999, British journal of Dermatology, Vol. 140, pp. 995–1009. DOI: 10.1046/j.1365-2133.1999.02898.x.*

41. UV exposure reduces immunization rates and promotes tolerance to epicutaneous antigens in humans: Relationship to dose, CD1a-DR+ epidermal macrophage induction, and Langerhans cell depletion. ***Cooper K.D., L. Oberheloman, T.A. Hamilton, 0. Baadsgaard, M. Terhune, G. Levee, T. Anderson, and H. Koren.*** *[ed.] Proc. Nati. Acad. Sci. USA. September 1992. Vol. 89, pp. 8497-8501.*

42. Effects of Ultraviolet Radiation on the immune systems in humans. ***Morison W.L,.*** *4, 1989, Photochem. and Photobiol., Vol. 50, pp. 515–524. DOI: 10.1111/j.1751-1097.1989.tb05557.x.*

43. Influence of season and latitude on the cutaneous synthesis of vitamin D3: Exposure to winter sunligght in Boston and Edmonton will not promote vitaminD3 synthesis in human skin. ***Webb A.R., L. Kline and M.F. Holick.*** *1988, J. Clin. Endocrinol. Metab., Vol. 67, pp. 373-378.*

44. Comparisons of estimated economic burdens due to insufficient solar ultraviolet irradiance and vitamin D and excess solar UV irradiance for the United States. ***Grant W.B., C.F. Garland and M.F. Holick.*** *2005, Photochem. Photobiol. , Vol. 81, pp. 1276-1286.*

45. UVR, vitamin D and three autoimmune diseases multiple sclerosis, type 1 diabetes, rheumatoid arthritis. ***Ponsonby A.L., R.M. Lucas and I.A. van der Mei.*** *2005, Photochem. Photobiol. , Vol. 81, pp. 1267-1275.*

46. Vitamin D status and arterial hypertension: a systematic review. . ***Pilz S., A. Tomaschitz, E. Ritz, T.R. Pieber, T.R.*** *2009, Nat. Rev. Cardiol., Vol. 6, pp. 621-630.*

47. Vitamin D for treatment and prevention of infectious diseases: a systematic review of randomized controlled trials. ***Yamshchikov A.V., N.S. Desai, H.M. Blumberg, T.R. Ziegler, V. Tangpricha.*** *2009, Endocr. Pract. , Vol. 15, pp. 438-449.*

48. Sunlight, UV-radiation, vitamin D and skin cancer: how much sunlight do we need? ***Holick M.F.,*** *2008, Adv. Exp. Med. Biol., Vol. 624, pp. 1-15.*

49. Ultraviolet exposure scenarios: risks of erythema from recommendations on cutaneous vitamin D synthesis. . ***Webb A.R. and O. Engelsen.*** *2008, Adv. Exp. Med. Biol., Vol. 624, pp. 72-85.*

50. Calculated ultraviolet exposure levels for a healthy vitamin D status. ***Engelse O.and A.R. Webb.****, 2006, Photochem. and Photobiol., Vol. 82, pp. 1697-703.*

51. http://middlepath.com.au/qol/sunlight_vitamin-D_skin-cancer_suntan_sunburn.php. [Online]

52. Clothing prevents ultraviolet-B radiation-dependent photosynthesis of vitamin D. ***Matsuoka L.Y., Wortsman J., Dannenberg M.J., Hollis B.W., Lu Z. and Holick M.F.*** *1992, Journal of Clinical Endocrinology and Metabolism, Vol. 75, pp. 1099-1103.*

53. Physics concepts of solar ultraviolet radiation by distance education. ***Parisi A.V.,*** *2005, Eur. J. Phys. , Vol. 26, pp. 313–320.*

54. Decreased bioavailability of vitamin D in obesity. ***Wortsman J., L.Y. Matsuoka, T.C. Chen, Z. Lu, and M.F. Holick.*** *2000, Am. J. Clin. Nutr., Vol. 72, pp. 690-3.*

55. Spectral character of sunlight modulates photosynthesis of previtamin D3 and its photoisomers in human skin. ***MacLaughlin J.A., R.R. Anderson and M.F. Holick.*** *1982, Science, Vol. 216, pp. 1001–1003.*

56. Ultraviolet Radiation dosimetry with polysulhone film. ***Diffey B. L.,*** *[ed.] (New York: Academic). 1989, Radiation Measurement in Photobiology, pp. 135–59.*

57. Techniques for assessing human UV exposures. ***Kimlin M. G.,*** *San Diego, Aug : s.n., 2003. Proc. SPIE, Ultraviolet Ground and Space-Based Measurements, Models and Effects III. Vol. 5156 , pp. 197–206.*

58. Spectral UV irradiance on vertical surface: a case study. ***Webb A.R., Weihs P., and M. Blumthaler.*** *4, 1999, Photochem. Photobiol. , Vol. 69, pp. 464–470.*

59. Exposure to UV radiation and human health. ***Kimlin, M. G.*** *[ed.] Proc. San Diego : s.n., August 2005. Proc. SPIE, Ultraviolet Ground and Space based measurements models and effects V. p. 5886.*

60. Evidence of a possible turning point of UVB increase over Canada, Europe and Japan. ***Zerefos C. S., K. Tourpali, K. Eleftheratos, S. Kazadzis, C. Meleti, U. Felster, T. Koskela, A. Heikkila.*** *2011, Atmos. Chem. Phys. Discuss., Vol. 11, pp. 28545-28561.*

61. WMO: Scientific assessment of ozone depletion: 2010. ***World Meteorological Organization, Global Ozone Research and Monitoring Project.*** *2011. Techn. Rep.*

62. COST 726, Long Term Changes and Climatology of UV Radiation Over EuropeFinal Report. ***Litynska Z., P. Koepke and L. Vuilleumier.*** *Publication of the European Communities. Brussels, Belgium : s.n., 2010. Available at: http://www.cost726.org..*

63. Uncertainty evaluation of the spectral UV irradiance evaluated by using the UVSPEC Radiative Transfer Model. ***Cordero R.R., G. Seckmeyer, D. Pissulla, L. DaSilva and F. Labbe.*** *2007, Opt. Commun, Vol. 276, pp. 44-53. doi: 10.1016/j.optcom.2007.04.008.*

64. Towards closure between measured and modelled UV under clear skies at four diverse sites. ***Badosa J., R.L. McKenzie, M. Kotkamp, J. Calbó, J.A. González, P.V. Johnston, M. O'Neill, and D.J. Anderson,.*** *11, 2007, Atmos. Chem. Phys., Vol. 7, pp. 2817-2837.*

65. UNEP: Environmental effects of ozone depletion and its interactions with climate change: 2010 assessment. ***United Nations Environment Programme,*** *2010. Techn. Rep.*

66. Uncertainty of measurements of spectral UV irradiances. ***Seckmeyer G., and G. Bernhard.*** *1999, J. Geophys. Res, Vol. 104, pp. 14321-14346.*

67. On the Importance of Spectral Responsivity of Robertson-Berger type Ultraviolet RaRadiometers. ***di Sarra A., P.***

Disterhoft and J. DeLuisi. *2002 : s.n., Photochem. Photobiol., Vol. 76, pp. 64-72.*

68. Solar UV Dose Patterns in Italy. ***Meloni D., G. R. Casale, A. M. Siani, S. Palmieri and F. Cappellani.*** *6, 2000, Photochem. Photobiol., Vol. 71, pp. 681-690.*

69. Guidelines for Site Quality Control of Uv Monitoring. ***WMO.*** *126, s.l. : WMO/TD, 1998, Vol. 884.*

70. Traveling reference spectroradiometer for routine quality assurance of spectral solar ultraviolet irradiance measurements. ***Gröbner J., J. Schreder, S. Kazadzis, A. F. Bais, M. Blumthaler, P. Görts.*** *25, 2005, Appl. Opt., Vol. 44, pp. 5321-5331.*

71. http://www.pmodwrc.ch/euvc/euvc.html. *[Online]*

72. Temperature dependence of Brewer UV measurements at Rome station. ***Siani A.M., G. Benevento, G. R. Casale.*** *2003. Proc. The International Symposium on Optical Science and Technology, Ultraviolet Ground and Space based measurements, models and effects III. Vol. 5156, pp. 355-366.*

73. Comparison of total ozone and erythemal UV data from OMI with ground-based measurements at Rome station. ***Ialongo I., G. R. Casale, A. M. Siani.*** *2008, Atmos. Chem. Phys., Vol. 8, pp. 3283–3289.*

74. Report on Protocol of the intercomparison at the University of Rome La Sapienza, Italy on June 03 to 06, 2008 with the traveling reference spectroradiometer Qasume from PMOD/WRC. ***Hulsen G,.*** *2008.*

75. ***National Institute for Public health and the Environment,.****http://www.rivm.nl/en/environmentandchemicals/radiation/nonionisingradiation/shic/.* www.rivm.nl. *[Online]*

76. http://www.muk.uni-hannover.de/~seckmeyer/EDUCE/. [Online] 2000 ***Seckmeyer.***.

77. http://www.ozone.fmi.fi/SUVDAMA/. [Online]

78. http://www.woudc.org/. *[Online]*

79. http://es-ee.tor.ec.gc.ca/cgi-bin/totalozone. [Online]

80. The ozone monitoring instrument. ***Level P.F., G. H. J. van den Oord, M. R. Dobber, A. Malkki, H. Visser, J. de Vries, P. Stammes, J. Lundell, and H. Saari.*** *5, 2006, IEEE Trans. Geo. Rem. Sens., Vol. 44, pp. 1093–1101.*

81..
http://toms.gsfc.nasa.gov/aerosols/AI_definition/ai_ep_definition.pdf. ***(NASA), National Aeronautics and Space Administration*** *[Online]*

82. Derivation of aerosol properties from satellite measurements of backscattered ultraviolet radiation: Theoretical Basis. ***Torres O., P. K. Bhartia, J. R. Herman, Z. Ahmad, J. Gleason.*** *1998, J. Geophys. Res., Vol. 103, pp. 17099-17110.*

83. Report of the WMO-WHO Meeting of Experts on Standardization of UV Indices and their Dissemination to the Public. *Geneva-Switzerland : s.n., 1997. WMO/ TD-No.921. WMO/GAW Report No. 127* ***World Meteorological Organization.***.

84. International Standard Global Solar UV Index. *CIE Central Bureau. Vienna-Austria : s.n., 2003.* ***Commission Internationale de l'Eclairage (CIE),.*** *CIE Standard S 013:2003.*

85. Action UV Index for the Public. *European Communities. Brussels : s.n., 2000* ***,COST-713.***.

86.. Compte Rendu 9. *Cambridge : Cambridge University Press, 1937. pp. 596–625****(CIE), Commission Internationale de l'Eclairage***.

87. Optical Radiation Physics and Illuminating Engineering; Quantities and Symbols of Photobiologically Effective Radiation. ***Deutsches Institut fur Normung,.*** *Beuth Verlag Berlin/Koln : s.n., 1979. DIN5031-10.*

88. Know Your Standard: Clarifying the CIE Erythema Action Spectrum. ***Webb A. R., H. Slaper, P. Koepke and A.W. Schmalwieser.*** *2011, Photochem. Photobiol., Vol. 47, pp. 483–486. DOI: 10.1111/j.1751-1097.2010.00871.x.*

89. Action Spectrum for the Production of previtamin D3 in Human Skin. ***Bouillon R., J. Eisman, M. Garabedian, M. Holick, J. Kleinschmidt, T. suda, I. Terenetskaya and A. Webb.*** *Vienna : s.n., 2006, UDC, pp. 612.014.481-06. CIE.*

90. Calculations of the human vitamin D exposure from UV spectral measurements at three European stations. ***Kazantzidis A, A.F. Bais, M.M. Zempila, S. Kazadzis, P.N. den Outer, T. Koskela and Harry Slaper.*** *2009, Photochem. Photobiol., Vol. 8, pp. 45–51. DOI: 10.1039/b811216a.*

91. On the relationship between erythemal and vitamin D action spectrum weighted ultraviolet radiation. ***Fioletov V.E., L.J.B. McArthur, T.W. Mathews and L. Marrett b.*** *2008, Photochem. Photobiol., Vol. 95, pp. 9-16. doi:10.1016/j.jphotobiol.2008.11.014.*

92. Daily duration of vitamin D synthesis in human skin with relation to latitude, total ozone, altitude, gorund cover, aerosols and cloud thickness. ***Engelsen O., M. Brustad, L. Aksnes and E. Lund.*** *2005, Photochem. Photobiol., Vol. 81(6), pp. 1287-1290.*

93. Changes in biologically active ultraviolet radiation reaching the Earth's. ***Madronich S., R. L. McKenzie, L. O. Björn, and M. M. Caldwell.*** *1998, Photochem. Photobiol., Vol. 46, pp. 5-19.*

94.. Radiation amplification factors - improved formulation accounts for large increases in ultraviolet. [book auth.] P.A. Penhale (Eds.), C.S. Weiler. Ultraviolet Radiation in Antarctica: Measurements and Biological Effects. ***Madronich S and Booth C.R.,*** *Washington : American Geophysical Union, 1994, pp. 39-42.*

95. The atmosphere and UV-B radiation at ground level. ***Madronich S..*** *[book auth.] A.R. Young (Eds.) L.O. Bjorn.* Environmental UV Photobiology. *New York : s.n., 1993, pp. 1-39.*

96. —. UV radiation in the natural and perturbed atmosphere. [book auth.] M. Tevini (Ed). Environmental Effects of UV (Ultraviolet) Radiation. *Lewis : s.n., 1993, pp. 17-69.*

97. Estimation of optimal serum concentrations of 25-hydroxyvitamin D for multiple health outcomes. ***Bischoff-Ferrari H. A., E. Giovannucci, W. C. Willett, T. Dietrich and B. Dawson-Hughes.*** *2006, Am. J. Clin. Nutr., Vol. 84, pp. 18-28.*

98. Ultra-violet irradiation corrects vitamin D deficiency and suppresses secondary hyperparathyroidism in the elderly. ***Chel V.G.M., M. E. Ooms, C. Popp-Snijders, S. Pavel,A. A. Schothorst, C. C. E. Meulemans and P. Lips.*** *1998, J. Bone Miner. Res., Vol. 13, pp. 1238–1242.*

99. The urgent need to recommend an intake of vitamin D that is effective. ***Vieth R., H. Bischoff-Ferrari, B. J. Boucher, B. Dawson-Hughes,C. F. Garland, R. P. Heaney, M. F. Holick, B. W. Hollis,C. Lamberg-Allardt, J. J. McGrath, A. W. Norman, Robert.Scragg, S. J. Whiting, W. C. Willett and A. Zittermann.*** *2007, Am. J. Clin. Nutr., Vol. 85, pp. 649–650.*

100.. Clarifying the vitamin D controversy: The health benefits of supplementation by diet versus sunshine. ***Gilchrest D., and B.A. Wolpowitz*** *[book auth.] Edited by B. A. Gilchrist and J.*

Krutmann. Skin Aging. *Berlin Heidelberg : Springer, 2006, pp. 81-102.*

101. Vitamin D: The underappreciated D-lightful hormone that is important for skeletal and cellular health. ***Holick, M. F.*** *2002, Curr.Opin. Endocrinol. Diab., Vol. 8, pp. 87-98.*

102. Possible dosimeter for ultraviolet radiation. ***Davis A., G H.W.Deane, B.L.Diffey.*** *1976, Nature, Vol. 261, pp. 169-170 .*

103. Techniques for assessing human UV exposures. ***Kimlin, M. G.*** *2003. Ultraviolet Ground and Space based measurements, models and effects III. Vols. Proc. SPIE 5156, 197, pp. 197-206. doi:10.1117/12.509096.*

104. Personal ultraviolet radiation dosimetry with polysulphone film badges. ***Diffey, B.L.*** *1984, Photodermatol., Vol. 1, pp. 151–7.*

105. Ultraviolet film badges for personal exposure studies. ***Diffey, B.L.*** *5, 1996, Photodermatology, Photoimmunology & Photomedicine, Vol. 12, p. 224. DOI: 10.1111/j.1600-0781.1996.tb00207.x.*

106. Variability among polysulphone calibration curves. ***Casale G.R., M. Borra, A. Colosimo, M. Colucci, A. Militello.*** *2006, Phys. Med. Biol., Vol. 51, pp. 4413–4427. doi:10.1088/0031-9155/51/17/019.*

107. Determination of the calibration factor of polysulphone film UV dosemeters for terrestrial solar radiation. ***Krins A., B. Dorschel,P. Knuschke, H.K. Seidlitz and S. Thiel.*** *2001, Radiat. Prot. Dosim., Vol. 95, pp. 345–52.*

108. Total ozone and surface UV trends in the United Kingdom: 1979–2008. ***Smedley A. R. D., J. S. Rimmer, D. Moore, R. Toumi, A. R. Webb.*** *International Journal of Climatology. DOI: 10.1002/joc.2275.*

109. hhttp://www.woudc.org/data/summaries_e.html. [Online]

110. Solar UV-B irradiance and total ozone in Italy: Fluctuations and trends. ***Casale G. R., D. Meloni, S. Miano, S. Palmieri, A.M. Siani.*** *D4, 2000, J. Geophys. Res., Vol. 105, pp. 4895-4901.*

111. Action Spectrum for the Production of previtamin D3 in Human Skin. ***Bouillon R., J. Eisman, M. Garabedian, M. Holick, J. Kleinschmidt, T. suda, I. Terenetskaya and A. webb.*** *Vienna : s.n., 2006, UDC, pp. 612.014.481-06. CIE.*

112. ***COST-713.*** Action UVB Forecasting. *European Communities. Brussels : s.n., 2000.*

113. Statistical power analysis for the behavioral sciences. ***Cohen JW.,.*** *s.l. : 2nd edn. Hillsdale, NJ: Lawrence Erlbaum Associates., 1988.*

114. Sensitivity of Biologically Active UV Radiation to Stratospheric Ozone Changes: Effects of Action Spectrum Shape and Wavelength Range . ***Micheletti M.I., R.D. Piacentini and S. Madronich.*** *5, 2003, Photochem. and Photobiol., Vol. 78 , pp. 456–461.*

115. EUV change over Korean peninsula. ***Cho H., JS Lee.*** *Korea : s.n., 2001. Proceeding of Korea Meteorological Society. Vol. 11(1), pp. 510-513.*

116. Use of an improved radiation amplification factor to estimate the effect of total ozone changes on action spectrum weighted irradiances and an instrument response function. ***Herman J.R..*** *2010, J. Geophys. Res., Vol. 115. doi:10.1029/2010JD014317.*

117. www.epicentro.iss.it. [Online]

118. UV radiation: Balancing Risks and Benefits. ***McKenzie R. L., J. B. Liley and L. O. Bjorn.*** *2008, Photochem. Photobiol. DOI: 1.1111/j.1751-1097.2008.00400.x.*

119. UV radiation: balancing risks and benefits. ***McKenzie R. L., J. B. Liley, L.O. Bjorn.*** *2009, Photochem Photobiol., Vol. 85, pp. 88-98.*

120. ***Ahmad S. P., O. Torres, P. K. Bhartia, G. Leptoukh, S. Kempler.*** Aerosols Index from TOMS and OMI measurements. *NASA Goddard Space Flight Center. Greenbelt, USA : s.n.*

121. Action spectrum conversion factors that change erythemally weighted to pre-vitamin D3 weighted doses. ***Pope S. J., M. F. Holick, S. Mackin, D. E. Godar.*** *2008, Photochem. Photobiol, Vols. doi:10.1111/j.1751-1097.2008.00373x.*

122. Joint ISO / CIE Standard:Erythema Reference Action Spectrum and Standard Erythema Dose. ***International Organization for Standardization / Commission Internationale de l'Eclairage,.*** *CIE Central Bureau. Vienna, Austria : s.n., 1999. ISO 17166/CIE S007/E-1999.*

123. Ultraviolet-B radiation increases serum 25-hydroxyvitamin D levels: The effect of UVB dose and skin color. ***Armas L. A. G., S. Dowell, M. A. RN, S. Duthuluru, C. Huerte, B. W. Hollis, R. Lund and R. P. Heaney.*** *2007, J. Am. Acad. Dermatol., Vol. 57, pp. 588 - 593.*

124. The importance of the depth distribution of melanin in skin for DNA protection and other photobiological processes. ***Nielsen K. P., L. Zhao, J. J. Stamnes, K. Stamnes and J. Moan.*** *2006, J. Photochem. Photobiol., Vol. B 82, pp. 194–198.*

125. Surface ultraviolet radiation. ***Kerr J.B., V. E. Fioletov.*** *2008, Atmos.-Ocean, Vol. 46, pp. 159-184. doi: 10.3137/ao.460108.*

126. Comparing ground-level spectrally resolved solar UV measurements using various instruments: A technique

resolving effects of wavelenght shift and slit width. ***Slaper H., H. A. J. M. Reinem, M. Blumthaler, M. Huber and F. Kuik.*** *1860-1877, 1996, J. Appl. Meteorol., Vol. 35(10).*

127. Uncertainty of measurements of spectral solar UV irradiance. ***Bernhard G., G. Seckmeyer.*** *1999, J. Geophys. Res., Vol. 12, pp. 14 321–14 345.*

128. International response to the challenge of measuring solar ultraviolet radiation. ***Weatherhead E. C., A. R. Webb.*** *1997, Radiat. Protection Dosimetry, Vol. 72, pp. 223-229.*

129. A photoelectric spectrophotometer for measuring the amount of atmospheric ozone. ***Dobson, G. M. B.*** *1931, Proc. Phys. Soc. London, Vol. 43, pp. 324-337.*

130. ***Diffey A.F., B.L. McKinlay,*** *A reference action spectrum for ultra-violet induced erythemal in human skin. [ed.] W. F. Passchier and B. F. Bosnjakovic.* Human Exposure to Ultraviolet Radiation: Risks and Regulations. *s.l. : Elsevier, 1987, pp. 83-87.*

131. A replacement for the Dobson spectrophotometer? ***Brewer A. W.,*** *1973, Pure Appl. Geophys., Vols. 106-108, pp. 919-927.*

132. Comparison of biologically effective spectra for erythema and pre-vitamin D3 syntesis. ***Parisi A.V., D. J. Turnbull, J. Turner.*** *2009, Int. J. Biometeoroll, Vol. 53, pp. 11-15.*

133. Validation of OMI products over Europe with ground-based UV instruments. ***Bais A., A. Kazantzidis, S. Kazadzis, M. Zempila.*** *[ed.] Contribution from Aristotle University of Thessaloniki. 4, 2007, OMI AO Progress Report, pp. 66-88. available at http://www.knmi.nl/omi/research/validation/ao/.*

134. ***Geiss O.,*** Manual for Polysulphone Dosimeters: Characterisation, Handling and Application as Personal UV Exposure Devices. *s.l. : European Communities, 2003.*

*135*Scientific Assessment of Ozone Depletion: 1994. . ***WMO (World Meteorological Organization),.*** *Geneva, Switzerland : s.n., 1994.*

136. Traveling reference spectroradiometer for routine quality assurance of spectral solar ultraviolet irradiance measurements. ***Gröbner J., J. Schreder, S. Kazadzis, A. F. Bais, M. Blumthaler, P. Görts.*** *25, 2005, Appl. Opt., Vol. 44, pp. 5321-5331.*

137. Comparison of total ozone and erythemal UV data from OMI with ground-based measurements at Rome station. ***Ialongo I., G. R. Casale, A. M. Siani.*** *2008, Atmos. Chem. Phys., Vol. 8, pp. 3283–3289.*

138. Temperature dependence of Brewer UV measurements at Rome station. ***Siani A. M., G. Benevento, G. R. Casale.*** *2003. Proc. The International Symposium on Optical Science and Technology, Ultraviolet Ground and Space based measurements, models and effects III. Vol. 5156, pp. 355-366.*

139. Derivation of aerosol properties from satellite measurements of backscattered ultraviolet radiation: Theoretical Basis. ***Torres O., P. K. Bhartia, J. R. Herman, Z. Ahmad, J. Gleason.*** *1998, J. Geophys. Res., Vol. 103, pp. 17099-17110.*

140. Influence of season and latitude on the cutaneous synthesis of vitamin D3: exposure to winter sunlight in Boston and Edmont will not promote vitamin D3 synthesis in human skin. ***Webb. A. R., L. Kline, M. F. Holick.*** *1988, J. Clin. Endocrinol. Metab., Vol. 67, pp. 373-378.*

141. Changes in biologically active ultraviolet radiation reaching the Earth's. ***Madronich S., R. L. McKenzie, L. O. Björn, and M. M. Caldwell.*** *1998, Photochem. Photobiol., Vol. 46, pp. 5-19.*

142. ***Madronich, S.*** *UV radiation in the natural and perturbed atmosphere. [book auth.] M. Tevini (Ed).* Environmental Effects of UV (Ultraviolet) Radiation. *Lewis : s.n., 1993, pp. 17-69.*

143. —. The atmosphere and UV-B radiation at ground level. [book auth.] A.R. Young (Eds.) ***L.O. Bjorn****.* Environmental UV Photobiology. *New York : s.n., 1993, pp. 1-39.*

144. ***Booth C.R., S. Madronich.*** *Radiation amplification factors - improved formulation accounts for large increases in ultraviolet. [book auth.] P.A. Penhale (Eds.), C.S. Weiler.* Ultraviolet Radiation in Antarctica: Measurements and Biological Effects. *Washington : American Geophysical Union, 1994, pp. 39-42.*

145. Vitamin D deficiency. ***Holick M. F.,*** *2007, N. Engl. J. Med., Vol. 357, pp. 266-281.*

146. Estimation of optimal serum concentrations of 25-hydroxyvitamin D for multiple health outcomes. ***Bischoff-Ferrari H.A, E. Giovannucci, W. C. Willett, T. Dietrich and B. Dawson-Hughes.*** *2006, Am. J. Clin. Nutr., Vol. 84, pp. 18-28.*

147. Ultra-violet irradiation corrects vitamin D deficiency and suppresses secondary hyperparathyroidism in the elderly. ***Chel V.G.M., M.E. Ooms, C. Popp-Snijders, S. Pavel,A. A. Schothorst, C. C. E. Meulemans and P. Lips.*** *1998, J. Bone Miner. Res., Vol. 13, pp. 1238–1242.*

148. The urgent need to recommend an intake of vitamin D that is effective. ***Vieth R., H. Bischoff-Ferrari, B. J. Boucher, B. Dawson-Hughes,C. F. Garland, R. P. Heaney, M. F. Holick, B. W. Hollis,C. Lamberg-Allardt, J. J. McGrath, A. W. Norman, Robert.Scragg, S. J. Whiting, W. C. Willett and A. Zittermann.*** *2007, Am. J. Clin. Nutr., Vol. 85, pp. 649–650.*

149. ***Gilchrest D., and B.A. Wolpowitz*** *Clarifying the vitamin D controversy: The health benefits of supplementation by diet versus sunshine. [book auth.] Edited by B. A. Gilchrist and J. Krutmann.* Skin Aging. *Berlin Heidelberg : Springer, 2006, pp. 81-102.*

150. http://es-ee.tor.ec.gc.ca/cgi-bin/totalozone. [Online]